Taylor & Francis
Taylor & Francis Group

Check for updates

New Pliocene right whale from Belgium informs balaenid phylogeny and function

Guillaume Duboys de Lavigerie[a,b]*, Mark Bosselaers[a,c], Stijn Goolaerts[a,d] iD, Travis Park[e,f] iD,
Olivier Lambert[a] iD and Felix G. Marx[a,b,g] iD

[a]*Directorate of Earth and History of Life,, Royal Belgian Institute of Natural Sciences (RBINS), Brussels, Belgium;* [b]*Department of Geology, University of Liège, Belgium;* [c]*Royal Zeeland Scientific Society, Middelburg, The Netherlands;* [d]*Scientific Heritage Service, RBINS, Brussels, Belgium;;* [e]*Department of Earth Sciences, University of Oxford, Oxford, UK;* [f]*Department of Life Sciences, Natural History Museum, London, UK;* [g]*Museum of New Zealand Te Papa Tongarewa, Wellington, New Zealand*

Right whales (Balaenidae) are the most distinctive family of extant baleen whales, thanks to their highly arched rostrum, tall lips and robust body shape. They are also the oldest, originating as much as 20 million years ago (Ma). Nevertheless, their fossil record is patchy and frequently understudied, obscuring their evolution. Here, we describe a new stem balaenid, *Antwerpibalaena liberatlas*, from northern Belgium, adding to the rich but historically problematic baleen whale assemblage of the Pliocene North Sea. Within right whales, *Antwerpibalaena* forms a clade with two previously described extinct genera, *Balaenella* and *Balaenula*. The holotype preserves much of the postcranial skeleton, and informs the emergence of typical balaenid traits like fused neck vertebrae and paddle-shaped flippers. Its size is intermediate between that of extant right whales and most of their extinct forebears revealing a more complex pattern of balaenid size evolution than previously thought.

http://zoobank.org/urn:lsid:zoobank.org:pub:A0070739-C6A3-42DE-B0A4-B309EF18DAFE

Keywords: Balaenidae; gigantism; cervical vertebrae; ear bones; forelimb; phylogeny

Introduction

Baleen whales (Mysticeti) are amongst the most peculiar of all living mammals. Their defining feature is the replacement of teeth by a row of comb-like keratinous plates (baleen), which they use to filter tiny prey directly from seawater (Pivorunas 1979). Their ranks include the largest animals that ever lived, and together with sperm whales they play a crucial role as ecosystem engineers (Roman *et al.* 2014). Right whales (Balaenidae) are one of the three main extant mysticete lineages, represented today by the Arctic bowhead whale, *Balaena mysticetus*, and three morphologically cryptic species inhabiting the North Atlantic (*Eubalaena glacialis*), North Pacific (*E. japonica*) and Southern Hemisphere (*E. australis*), respectively (McLeod *et al.* 1993; Gaines *et al.* 2005).

All right whales are characterized by elongate, finely fringed baleen accommodated inside a highly arched rostrum. This arrangement maximizes the surface available for filtration, and allows them to skim feed on tiny zooplankton, in particular copepods (Lambertsen *et al.* 2005; Werth & Potvin 2016). Other notable features include completely fused neck vertebrae; broad, paddle-like flippers; the lack of a dorsal fin; and several 'records' among cetaceans, such as the thickest blubber, the thickest skin, the greatest longevity, the longest baleen and the greatest head-to-body ratio (Westgate & Whitmore 2002; Bisconti 2003; George *et al.* 2017). Finally, all of the extant species are noticeably large, with total body lengths ranging from 13 to 19 m (George *et al.* 2017; Kenney 2017).

The origins and phylogeny of right whales remain controversial. While most recent studies interpret them as early diverging chaeomysticetes (Steeman 2007; El Adli *et al.* 2014; Boessenecker & Fordyce 2015; Bisconti *et al.* 2017; Buono *et al.* 2017; Marx *et al.* 2019), others advocate a more close-knit mysticete crown group excluding most extinct species (Geisler & Sanders 2003; Bouetel & de Muizon 2006; Deméré *et al.* 2008; Geisler *et al.* 2011; Churchill *et al.* 2012). Equally problematic is the relationship of balaenids with the pygmy right whale, *Caperea marginata*. Though traditionally regarded as close relatives (Bouetel & de Muizon 2006; Steeman 2007; Churchill *et al.* 2012; El Adli *et al.* 2014; Bisconti 2015; Boessenecker & Fordyce 2015; Berta & Deméré 2017; Bisconti *et al.* 2017), molecular and some morphological studies

---

*Corresponding author. Email: gduboysdelavigerie@yahoo.com

instead group *Caperea* with rorquals, grey whales and, sometimes, cetotheriids (McGowen *et al.* 2009; Steeman *et al.* 2009; Fordyce & Marx 2013; Gol'din & Steeman 2015; Marx & Fordyce 2015, 2016; Buono *et al.* 2017; McGowen *et al.* 2019). Finally, phylogenetic uncertainty persists even within Balaenidae, with the position of the earliest diverging species remaining particularly unstable (Bisconti 2005; Marx & Fordyce 2015; Bisconti *et al.* 2017; Buono *et al.* 2017).

At least some of these discrepancies may be rooted in the surprisingly small number of described balaenid fossils. The oldest unambiguous balaenid, *Morenocetus parvus*, dates to the early Miocene, around 20 Ma (Buono *et al.* 2017). Much of the subsequent fossil record remains cryptic, with only one species, *Peripolocetus vexillifer*, known from the middle Miocene (Deméré & Pyenson 2015). Specimens abruptly increase in abundance during the late Miocene, with records from Japan (Kimura 2009), Argentina (Cione *et al.* 2011), Australia (Fitzgerald 2004; Piper *et al.* 2006) and the USA (Barnes 1977). To date, however, much of this material remains understudied or entirely undescribed. Apparent balaenid diversity reached its peak during the Pliocene, but then drastically fell around 3 Ma, leaving only the two surviving genera (Kimura 2009; Marx & Fordyce 2015).

Among the localities that have yielded right whales, temporary exposures around the Belgian city of Antwerp and nearby areas in the southern Netherlands are particularly rich in Neogene cetacean fossils (Bosselaers *et al.* 2004; Bisconti 2005, 2015; Lambert & Gigase 2007; Lambert 2008a, b; Colpaert *et al.* 2015; Bisconti *et al.* 2017; Marx *et al.* 2019). The mid-Miocene to Pliocene cetacean assemblage of this region has been intensively studied since the nineteenth century (Van Beneden 1872; Abel 1938, 1941; Steeman 2010), which sometimes poses a challenge in the context of modern palaeontological practice. Though abundant, much of the recovered material lacks detailed locality and age information, and several supposed species are based on dubiously associated finds (Steeman 2010). As a result, the contribution of the Belgian record to a broader understanding of cetacean (and, specifically, mysticete) evolution has, until recently, been limited. Here, we describe a new Pliocene right whale from the vicinity of Antwerp, and discuss its implications for balaenid phylogeny and ecology.

Material and methods

Institutional abbreviations
IRSNB: Institut royal des Sciences naturelles de Belgique, Brussels, Belgium; **NMNS**: National Museum of Nature and Science, Tokyo/Tsukuba, Japan; **NMNZ**: Museum of New Zealand Te Papa Tongarewa, Wellington, New Zealand; **OCPC**: The Cooper Center, Orange County, USA; **OU**: Geology Museum, University of Otago, Dunedin, New Zealand; **USNM**: National Museum of Natural History, Smithsonian Institution, Washington DC, USA; **ZMT**: Canterbury Museum, Christchurch, New Zealand; **ZMUC**: Zoological Museum of the University of Copenhagen, Denmark.

Discovery and geological setting
Specimen IRSNB M2325 was discovered by one of the authors (SG) in 2013 at −10.4 m TAW (Tweede Algemene Waterpassing) depth, during construction of the northern door of the Kieldrecht Lock (previously known as the Deurganckdoksluis; 51°16′47″N, 4°14′50″E) in the Port of Antwerp, Belgium (Fig. 1A).

The skeleton was found 5–10 cm above the base of the upper Pliocene Oorderen Sands Member (Lillo Formation, Fig. 1B), within a highly fossiliferous glauconitic sand layer densely packed with molluscs and, to a lesser extent, marine vertebrates. Worn shells, reworked sandstones, flints and phosphatic concretions identify this basal shelly unit as a transgressive lag deposit. Nevertheless, IRSNB M2325 was partially articulated and occurred at the same level as numerous unworn and articulated bivalves, suggesting little or no reworking. Parts of the skeleton were encased in a thin layer of friable, non-fossiliferous glauconitic sandstone of uncertain genesis. The occasional presence of shark bite marks and barnacles on the bones indicate exposure on the sea floor prior to burial.

Post-depositional load-casting caused the basal shelly unit to collapse into the underlying Kattendijk Formation, resulting in an undulating base of the bed with an amplitude of *c.* 1.5 m, and the breakage of all bones larger than 60 cm. Together with the abundance of shells and the tight schedule of the ongoing construction, this factor prevented the creation of a detailed excavation map, but photographs of the excavation process will be deposited with the specimen and are available on request.

Preparation, photography and description
The fossil was prepared mechanically using hand tools and air scribes. For photography, the basicranium and ear bones were coated with sublimated ammonium chloride. Photographs were then taken at various foci, and digitally stacked in Photoshop CS6. For standard views, the ear bones were oriented so that the fenestra vestibuli pointed exactly ventrally, and the main ridge
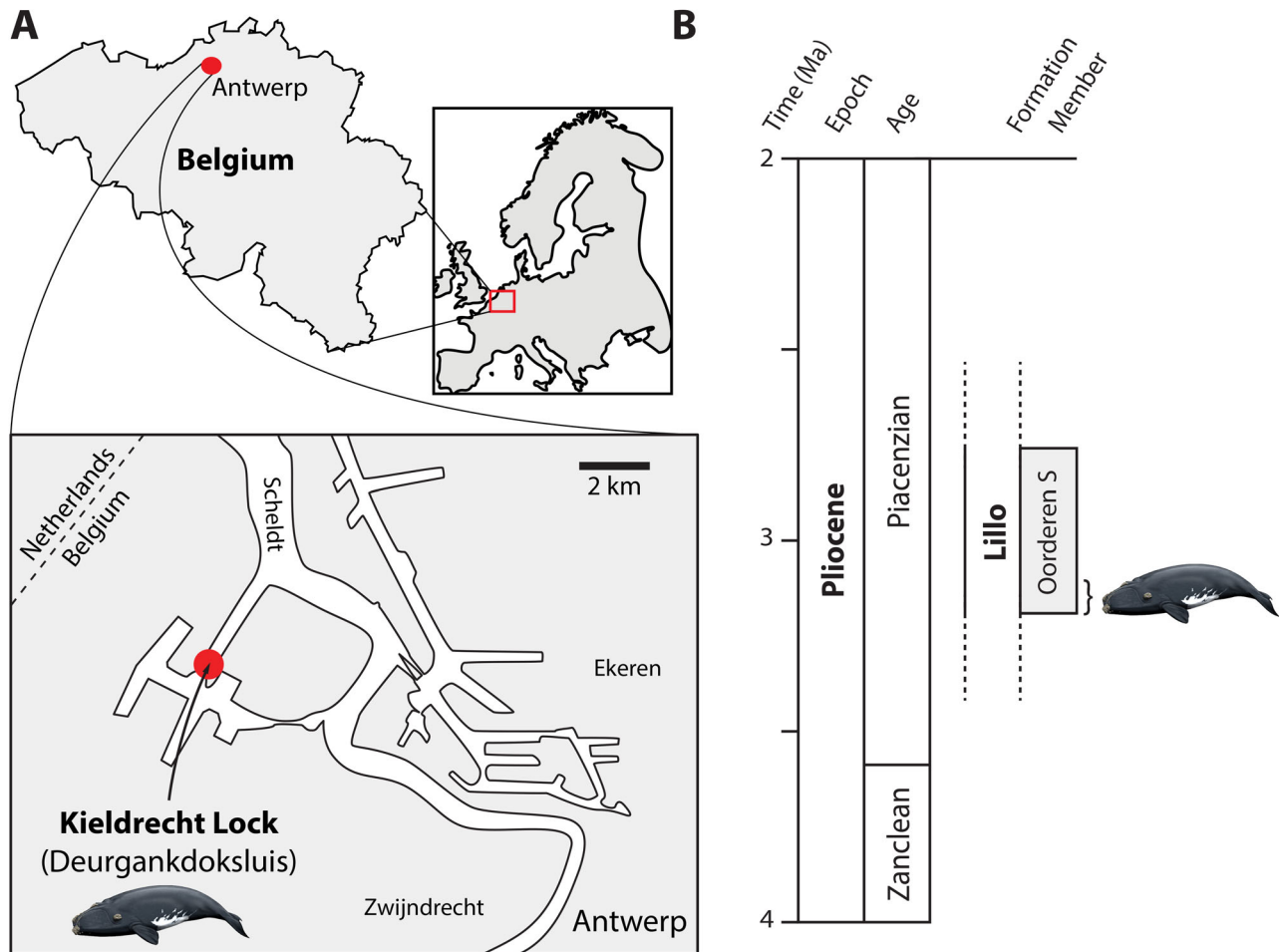
Figure 1. **A**, map and **B**, stratigraphic context of the type locality. Drawing of right whale by Carl Buell.

of the tympanic bulla exactly medially. Anatomical terminology follows Mead & Fordyce (2009).

CT scanning and 3 D reconstruction

We scanned the left periotic using an RX EasyTom (RX Solutions, Chavanod, France; http://www.rxsolutions.fr) computed tomography (CT) system, with a copper filter. Images were generated at a voltage of 120 kv and a current of 250 μA, with a set frame rate of 4.21 and an average of six frames. This generated 1440 images with a voxel size of 40.9183 μm. Reconstruction was performed using X-Act Software from RX Solutions. Based on these data, we then constructed a digital 3 D model of the bony labyrinth via the segmentation and thresholding editors in Avizo 9.0 (standard edition; Visualization Sciences Group, FEI). Three-dimensional mesh files are available on sketchfab (https://sketchfab.com/3d-models/be-rbins-new-genus-new-species-accepted-m-2325-90f2b9f8eaba4 d8286f6a35847d967ec) and from

the IRSNB http://virtualcollections.naturalsciences.be/; the full μCT data are available upon request.

Cochlear measurements, including height, width, volume, number of turns, cochlear canal length, extent of the secondary spiral lamina, the basal radius and the apical radius were taken following Park *et al.* (2017a). These measurements were then used to calculate several previously suggested ratios (Ketten & Wartzok 1990), including (i) the axial pitch (cochlear height/number of turns); (ii) the basal ratio (cochlear height/width); (iii) the cochlear slope (cochlear height/cochlear canal length/number of turns); and (iv) the radii ratio (basal radius/apical radius). Finally, we calculated the low-frequency hearing limit following Manoussaki *et al.* (2008):

$$f = 1507 \exp\left(-0.578[\rho - 1]\right) \qquad (1)$$

where f is the low frequency hearing limit at 60 dB re 20 μPa in air and 120 dB re 1 μPa in water, and ρ is the radii ratio value.

Estimation of body size

Total body length (TL) was estimated based on the bizygomatic width of the skull (BZW), using the 'stem mysticete' and 'stem balaenopteroid' equations of Pyenson & Sponberg (2011):

$$\log(\text{TL}) = 0.92 * \big(\log(\text{BZW}) - 1.72\big) + 2.68 \quad (2)$$

$$\log(\text{TL}) = 0.92 * \big(\log(\text{BZW}) - 1.64\big) + 2.67 \quad (3)$$

and the general mysticete equation of Lambert *et al.* (2010):

$$\text{TL} = 8.209 * \big(\text{BZW}\big) + 66.69 \quad (4)$$

Phylogenetic analysis

The new fossil was added to the total evidence matrix of Marx *et al.* (2019), resulting in a dataset comprising 110 taxa and 37,924 characters (37,647 molecular, 277 morphological). The full data matrix is available from MorphoBank (www.morphobank.org), project 3422. Following Marx *et al.* (2019), the morphological data were assigned a maximum-likelihood model (Lewis 2001) and a gamma parameter to allow for variable rates across traits (Mk + Γ). The coding bias was set to 'informative'. The complete matrix was analysed through the Cyberinfrastructure for Phylogenetic Research Science Gateway (CIPRES) (Miller *et al.* 2010), via a Markov chain Monte Carlo analysis implemented in MrBayes 3.2.6 (Ronquist *et al.* 2012). The analysis was run for 20 million generations and comprised three separate runs with four chains each. Convergence was assessed using the average standard deviation of split frequencies, aiming for ≤0.01. Results were sampled every 1000 generations, with the first 25% discarded as burn-in, and summarized in a consensus tree showing all compatible groups.

Systematic palaeontology

Cetacea Brisson, 1762
Neoceti Fordyce & de Muizon, 2001
Mysticeti Gray, 1864
Balaenidae Gray, 1821
Antwerpibalaena gen. nov.

Type species. *Antwerpibalaena liberatlas* gen. et sp. nov.

Diagnosis. As for the type and only species.

Derivation of name. Antwerp, after the city (Antwerpen in Flemish) that lends its name to the harbour area where the fossil was found and which has long been at the centre of Belgian cetacean research; *balaena*, Latin for whale.

Antwerpibalaena liberatlas sp. nov.
(Figs 2–14)

Diagnosis. Medium-sized right whale differing from all other chaeomysticetes except balaenids in having a notably twisted mandibular symphysis, a strongly hypertrophied lateral tuberosity and body of the periotic, a blade-like flange on the lateral tuberosity, and a small anterior process of the periotic with a rounded outline in medial view. Differs from all described balaenids in having an anteroposteriorly compressed external acoustic meatus delineated by a low, distally fading posterior meatal crest; further differs from *Balaenula*, *Balaenella*, *Balaenotus*, *Morenocetus* and *Peripolocetus* in its larger size; from *Morenocetus* and *Peripolocetus* in having a pointed, rather than bulbous, lateral tuberosity of the periotic bearing a blade-like flange; from *Peripolocetus* in having a transversely concave anteromedial portion of the tympanic bulla (in ventral view); from *Idiocetus guiccicardinii* in having a constricted, rather than massive, base of the compound posterior process of the tympanoperiotic; from *Balaenella*, *Balaenotus*, *Balaena mysticetus*, *Balaena ricei* and *Eubalaena* in having a larger hiatus Fallopii; from *Balaenula* in having a more acute Eustachian outlet and a flattened compound posterior process; from *Balaenella* in having a thicker main ridge of the tympanic bulla; from *Balaenotus* in having a less transversely concave anteromedial portion of the tympanic bulla (in ventral view); from *Balaena mysticetus*, *Balaena ricei* and *Eubalaena* in being smaller and in showing less hypertrophy of the periotic; and from *Balaena mysticetus*, *Balaena ricei* and extant *Eubalaena* spp. in having an unfused atlas.

Derivation of name. From *liber*, Latin for free; and atlas, after the name of the first cervical vertebra. The latter is unfused in the holotype of the new species.

Holotype. IRSNB M2325, comprising a fragmentary basicranium, both tympanoperiotics, the right auditory ossicles, both mandibles, parts of the hyoid apparatus, the right forelimb, all seven cervical vertebrae, five thoracic vertebrae, the sternum and several ribs.

Occurrence. The type and only specimen came from the Kieldrecht Lock (previously known as Deurganckdoksluis, Port of Antwerp area) on the left bank of the river Scheldt, north-west of the city of Antwerp, Belgium (Fig. 1). The specimen derives from the base of the Oorderen Sands Member (Lillo Formation), dated to 3.21–2.76 Ma (Piacenzian, late Pliocene) based on its dinoflagellate cyst assemblage (Louwye *et al.* 2004; De Schepper *et al.* 2009).

Description

Preservation and ontogenetic age
The cranium is highly fragmentary and heavily eroded, and comprises only a portion of the basicranium and the ear bones. The remaining elements of the skeleton are better preserved and essentially complete, but often broken into several sections. A thin, 1–2 mm thick concretionary layer covered much of the basicranium and the ear bones, and presumably helped the right auditory ossicles to stay in place. The epiphyses of the thoracic vertebrae and the humerus are fused, as are the basihyal and the thyrohyals. Together, these observations imply that the individual is an adult (Moran *et al.* 2015).

Cranium
In ventral view, the external acoustic meatus is notably narrow anteroposteriorly (6 mm at its proximal end) and delimited by a low, posteriorly convex and laterally fading posterior meatal crest (Fig. 2). The space enclosed by the external acoustic meatus and the exoccipital is narrow, in line with the flattened compound posterior process (Table 1). There is no distinct fossa for the sigmoid process of the tympanic bulla. Along the rim of the periotic fossa, just anterior to the anterior meatal crest, a series of transverse ridges and tubercles marks the articulation of the blade-like flange of the lateral tuberosity of the periotic with the squamosal.

The paroccipital process of the exoccipital is flat anteroposteriorly, and almost certainly did not project posterior to the (broken and missing) occipital condyle. A shallow sulcus is all that remains of the jugular notch. The sphenooccipital synchondrosis appears to be firmly fused, with no obvious trace of its former course. Anterior to the periotic fossa, the squamosal is broken but robust, consistent with the presence of posteroventrally oriented pterygoid and falciform processes as seen in extant balaenids (Fraser & Purves 1960, fig. 12f). The subtemporal crest is gently concave anteriorly, suggesting a transversely wide temporal fossa. The crest itself is smooth, with no obvious squamosal crease.

In anterior view, the base of the postglenoid process descends steeply from the level of the subtemporal crest. The process is too damaged to assess its morphology, but what is preserved suggests an elongate 'U'-shape (in posterior view) as in extant balaenids (Fig. 2). In anterolateral view, the squamosal bears two deep and clearly separated sutural surfaces for the parietal (dorsally) and the alisphenoid (ventrally), indicating that the latter was exposed on the outside of the cranium. There is no squamosal cleft.

Table 1. Measurements of the holotype of *Antwerpibalaena liberatlas* (IRSNB M2325), in mm. Vertebrae labels correspond to Figure 9.

Measurements	
Estimated bizygomatic width	1100–1200
Length of periotic, from lateral tuberosity to stylomastoid fossa	83
Length of compound posterior process	151
Maximum length of tympanic bulla	104
Width of tympanic bulla at sigmoid process	69
Height of mandible at mid-length	160
Length of mandible in a straight line	2670
Maximum width of atlas	245
Atlas, anteroposterior length of body	75
Fused axis–C7, anteroposterior length	104
Thoracic vertebra E, anteroposterior length of body	58
Thoracic vertebra F, anteroposterior length of body	69
Thoracic vertebra G, anteroposterior length of body	74
Thoracic vertebra H, anteroposterior length of body	101
?Thoracic vertebra I, anteroposterior length of body	136
Length of basihyal at midline	56
Length of humerus	295
Width of humerus mid-shaft, in lateral view	110
Length of radius	362
Width of radius mid-shaft, in lateral view	60
Length of ulna	400
Width of ulna mid-shaft, in lateral view	106

Periotic
In medial view, the anterior process is rounded and slightly shorter than the pars cochlearis (Fig. 3). The lateral tuberosity is hypertrophied and sharply pointed, and extends anteriorly beyond the anterior process. Near its base, the lateral tuberosity bears a ventrolaterally oriented, blade-like flange. The attachment of the tensor tympani is marked by a low, barely detectable ridge. The pars cochlearis is rounded ventrally, and longer anteroposteriorly than high dorsoventrally. The hiatus Fallopii is notably large, oval and located on the anterior face of the pars cochlearis, separate from the proximal opening of the facial canal. There is a well-defined median promontorial groove.

The fenestra cochleae is flush with the remainder of the pars cochlearis, rather than being recessed as in balaenopterids. The posterior cochlear crest is relatively short and bulges ventrally. The stylomastoid fossa is large and extends well posterior to the level of the pars cochlearis. Posteroventral to this fossa, and immediately dorsal to the facial sulcus, there is a second, sharply defined fossa of uncertain homology excavating the constricted base of the compound posterior process. The compound posterior process itself is flattened anteroposteriorly, and divided into a smooth ventral portion and a spongy dorsal plate.

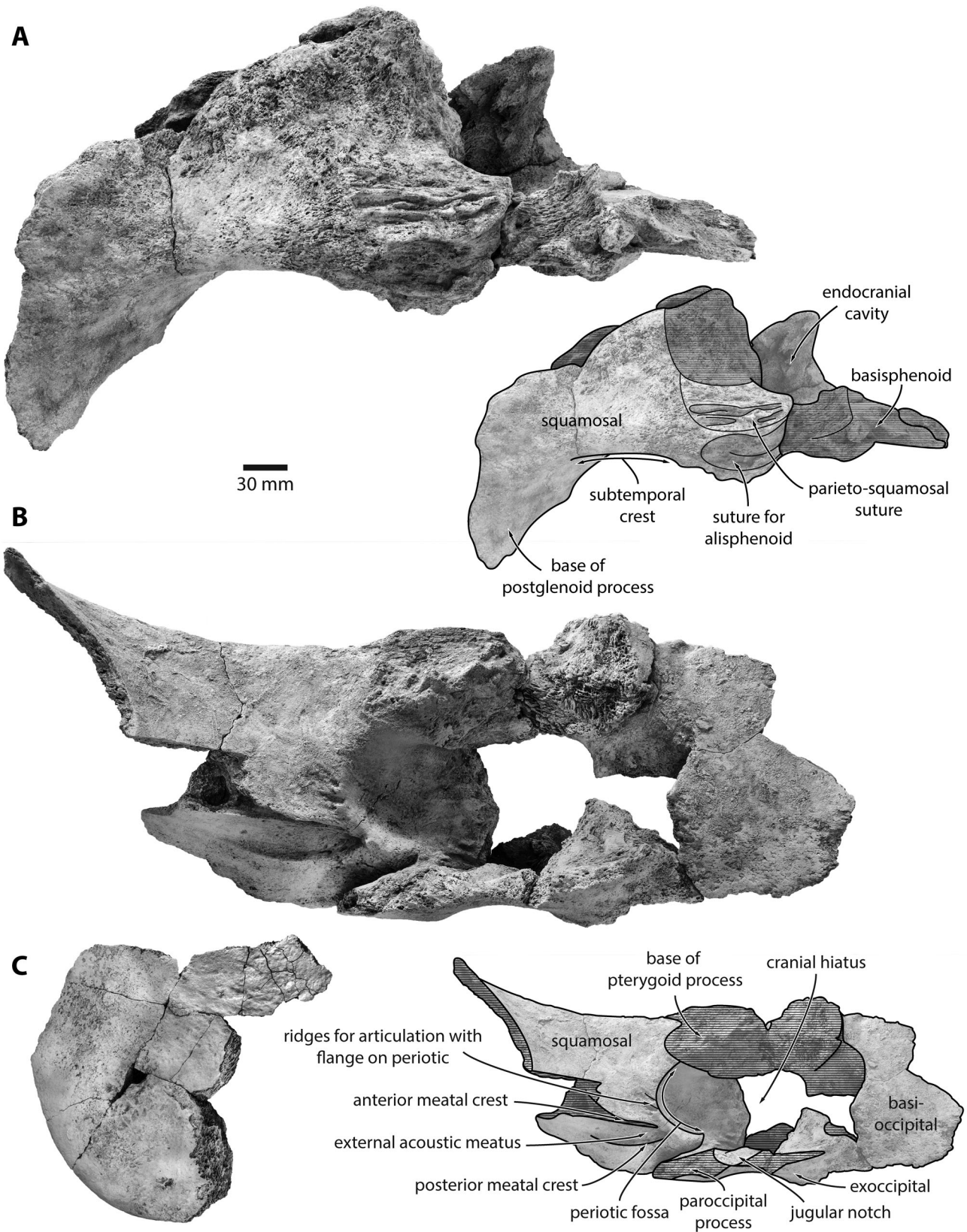In ventral view, the pars cochlearis is rounded (Fig. 4). The mallear fossa is indistinct, whereas the

Figure 2. Holotype skull of *Antwerpibalaena liberatlas* (IRSNB M2325). **A**, photograph and line drawing of the right squamosal in anterodorsolateral view. **B**, photograph and line drawing of the basicranium in ventral view. **C**, left postglenoid process in posterior views. Hatched parts are broken.
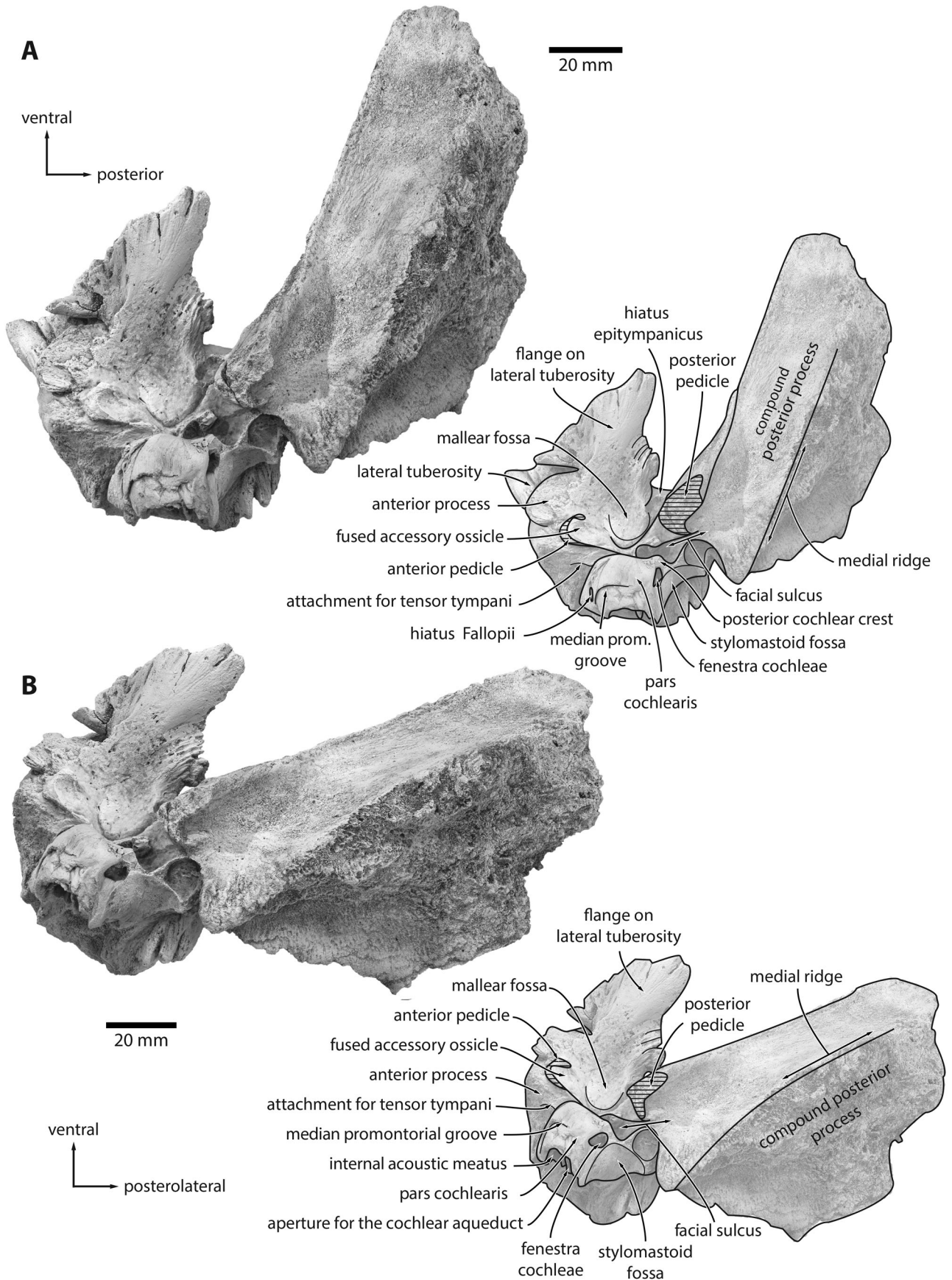
Figure 3. Holotype left periotic of *Antwerpibalaena liberatlas* (IRSNB M2325). Photographs and line drawings in **A**, medial and **B**, posterodorsomedial views. Hatched parts are broken.
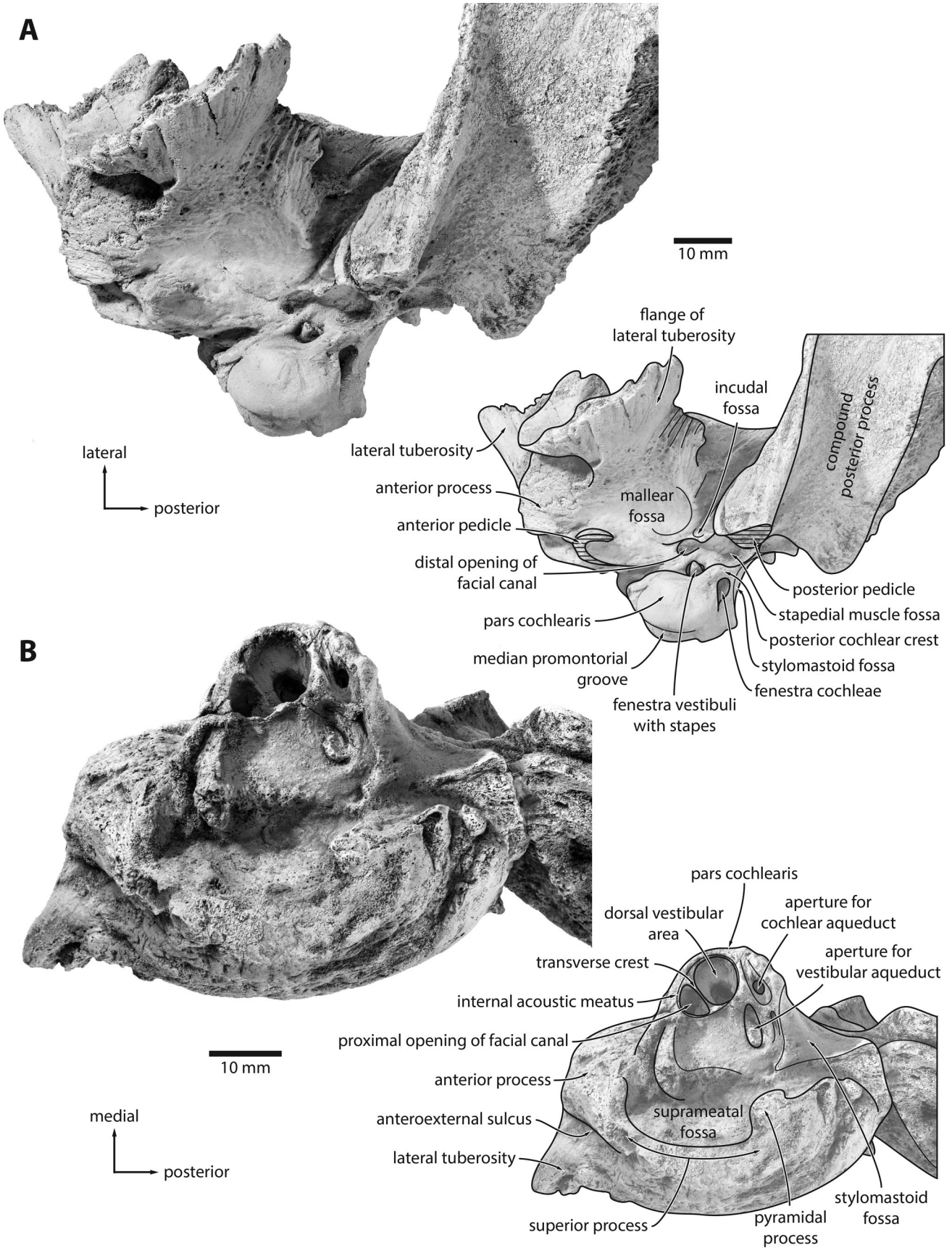
Figure 4. Holotype left periotic of *Antwerpibalaena liberatlas* (IRSNB M2325). Photographs and line drawings in **A**, ventral and **B**, dorsal views. Hatched parts are broken.
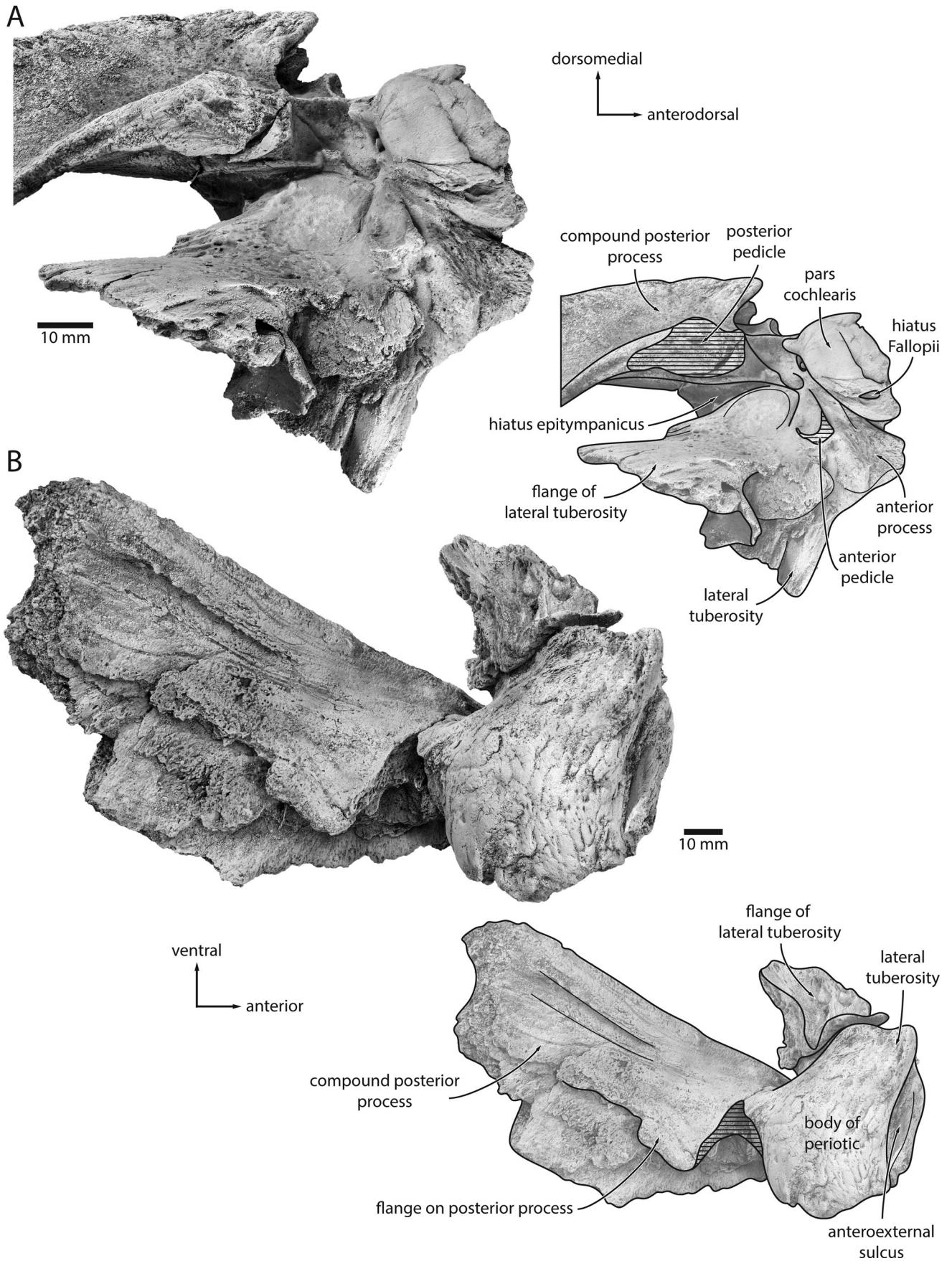
Figure 5. Holotype left periotic of *Antwerpibalaena liberatlas* (IRSNB M2325). Photographs and line drawings in **A**, anteroventromedial and **B**, lateral views.

Table 2. Measurements of the holotype left cochlea of *Antwerpibalaena liberatlas* (IRSNB M2325). See Park *et al.* (2017a) and Ketten & Wartzok (1990) for details on the various measurements.

Measurements	
number of turns	2.75
cochlear canal length (mm)	49.93
length of secondary spiral lamina (mm)	9.09
relative extent of secondary spiral lamina (%)	18.20
basal radius (mm)	7.73
apical radius (mm)	1.16
radii ratio	6.66
cochlear height (mm)	10.05
cochlear width (mm)	14.31
basal ratio (height/ width)	0.70
axial pitch (height/ number of turns)	3.65
cochlear slope (height/length of canal/number of turns)	0.07
cochlear volume (mm^3)	704.93

incudal fossa forms a well-defined pit. There is no squamosal flange. The anterior pedicle is fused to the periotic, with no visible trace of the fovea epitubaria. The pedicle is confluent, however, with a raised platform with well-defined anterior and medial borders, which presumably represents the remnant of the accessory ossicle. The facial sulcus is open both ventrally and posteriorly.

In dorsal view, there is a deep suprameatal fossa delineated by a low but clearly defined superior process (Fig. 4). The pyramidal process is located at the edge of this fossa, and confluent with the superior process. The transverse septum is thin and somewhat recessed into the internal acoustic meatus. The proximal opening of the facial canal is notably smaller than the dorsal vestibular area, with both being approximately circular. The aperture for the cochlear aqueduct is also circular, located medial to the slit-like aperture for the vestibular aqueduct, and not aligned with the internal acoustic meatus.

In posterior view, the fenestra cochleae is separated from the aperture for the cochlear aqueduct (Fig. 3). The compound posterior process tapers distally to a point, with no clearly defined surface that could be exposed on the lateral skull wall. In lateral view, the compound posterior process is mostly flat, except for a thin, dorsally oriented flange (Fig. 5). The blade-like flange of the lateral tuberosity is clearly separated from the remainder of the periotic by a deep groove. Anterior to the lateral tuberosity, there is a deep, somewhat oblique anteroexternal sulcus.

Cochlea

The left bony labyrinth is poorly preserved, with extensive damage to the basal portion of the cochlear canal,

vestibule and semicircular canals. The cochlea completes approximately 2.75 turns (Fig. 6; Table 2), and resembles that of *Eubalaena* and *Peripolocetus* in being tightly coiled and relatively tall (Ekdale & Racicot 2015; Ekdale 2016). As in other balaenids, there is no tympanal recess (Ekdale & Racicot 2015; Ekdale 2016; Park *et al.* 2017a, b). In vestibular view, the apical turn encloses a small open space and overlaps the section of the cochlear canal immediately below. In cross-section, the bone separating the basal turn from the apical turn is thin, as in other modern mysticetes. The secondary spiral lamina extends along the radial wall of the cochlear canal for 18% of its total length, similar to *Eubalaena* (15–22%), but less than in *Balaena* (30%) and *Peripolocetus* (34%) (Ekdale 2016; Park *et al.* 2017a). The radii ratio of 6.66 is lower than in *Eubalaena* and *Peripolocetus*, but somewhat higher than in *Balaena* (Ekdale & Racicot 2015; Ekdale 2016; Park *et al.* 2017a; Ritsche *et al.* 2018); see Ritsche *et al.* (2018) for a discussion of potential issues with this metric in cetaceans. Finally, the estimated low-frequency hearing limit is 57.07 Hz, lower than in *Balaena* (107 Hz), but higher than in *Eubalaena* (10–41 Hz) and *Peripolocetus* (12 Hz) (Ekdale 2016; Park *et al.* 2017a).

Tympanic bulla

In dorsal view, the anterior portion of the bulla is squared, giving the entire bone a box-like shape (Figs 7, 8). The Eustachian outlet is narrow, with its borders forming a somewhat acute angle. The involucral ridge runs parallel to, and largely at the same level as, the main ridge. Along its lateral rim, the involucrum bears several well-defined transverse creases. The floor of the tympanic cavity is smooth, with no transverse ridge dividing it into anterior and posterior halves. The tympanic sulcus forms a well-defined, 'U'-shaped shelf originating at the posterior pedicle, from where it dives ventrally beneath the junction between the conical and sigmoid processes. Overall, the bulla does not extend posteriorly beyond the level of the posterior pedicle.

In lateral view, the internal surface of the posterior pedicle is excavated by a dorsally oriented lobe of the tympanic cavity. The conical process is low and not overhung by the sigmoid process. The sigmoid cleft is shallow and largely vertical, so that there is no ventral border of the sigmoid process. The lateral furrow is deep, widens ventrally and is oriented obliquely, with its dorsal end located more posteriorly.

In medial view, the posterior face of the involucrum is flattened and faces posterodorsally. The main and involucral ridges are roughly parallel and remain widely separated along the entire length of the bulla. The area between the two ridges is pitted, suggesting the
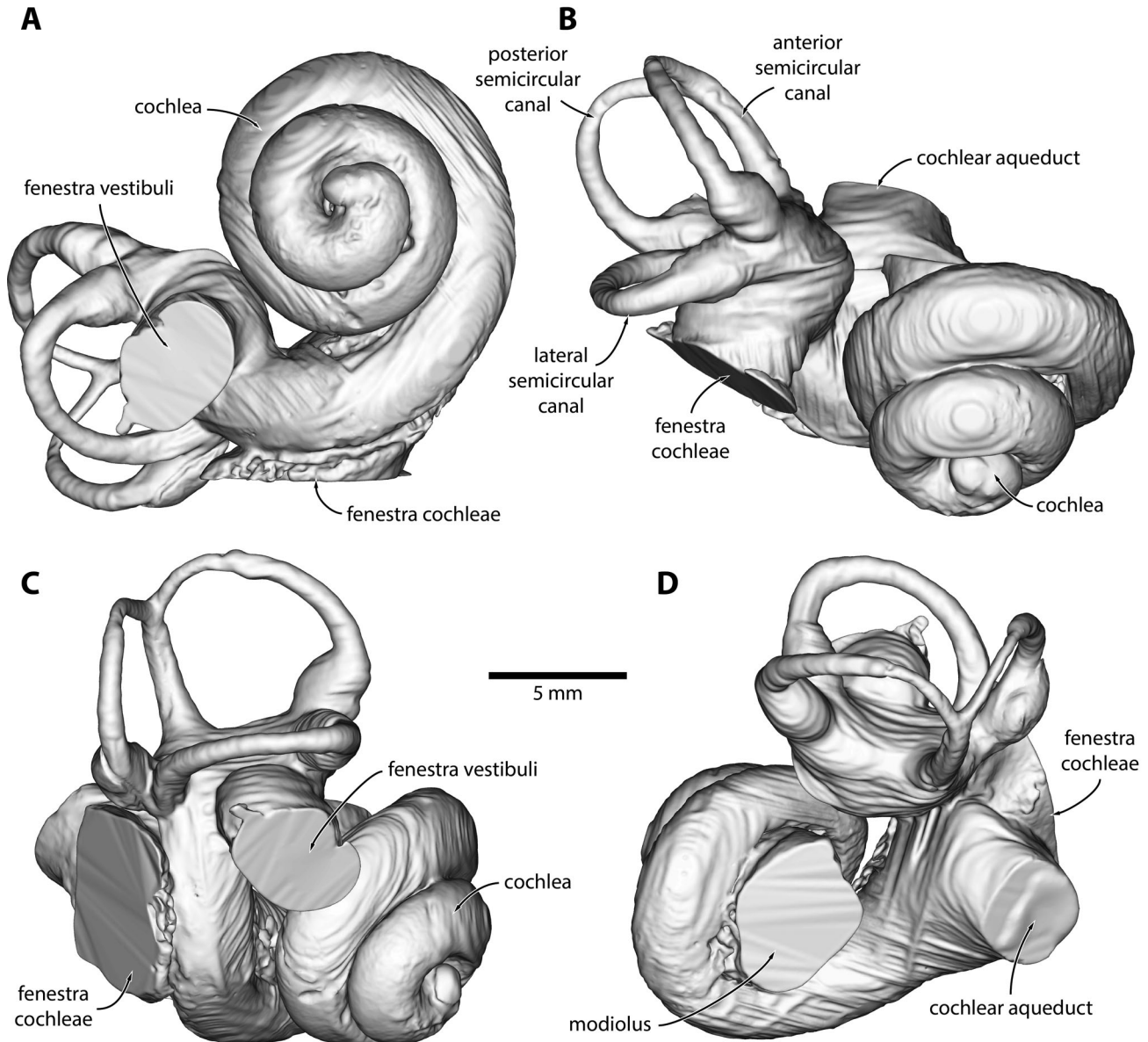
Figure 6. Holotype left bony labyrinth of *Antwerpibalaena liberatlas* (IRSNB M2325) in **A**, vestibular, **B**, anterior, **C**, lateral and **D**, dorsal views.

attachment of connective tissue between the bulla and the adjacent basioccipital crest. There is no median furrow. In posterior view, there is no clearly defined inner posterior prominence, with the dorsal surface of the involucrum instead being relatively low. There is no elliptical foramen. In anterior view, the lateral border of the sigmoid process is approximately vertical. The dorsal margin of the process is squared, with its dorsomedial corner remaining distinct from the anterior process of the malleus. In ventral view, there is an elongate, anteriorly widening depression that excavates much of the ventromedial surface on the bulla. Adjacent to this depression, the anteromedial corner of the bulla bears a series of short ridges and troughs. When viewed *in situ* (Fig. 9), the bullae are oriented such that their long axes converge anteriorly.

Auditory ossicles

The right stapes, incus and malleus are articulated and preserved *in situ* (Fig. 10). The anterior process of the malleus is broken where it joins the head, but appears to have been anteriorly excavated by the groove for the chorda tympani. The tubercule is
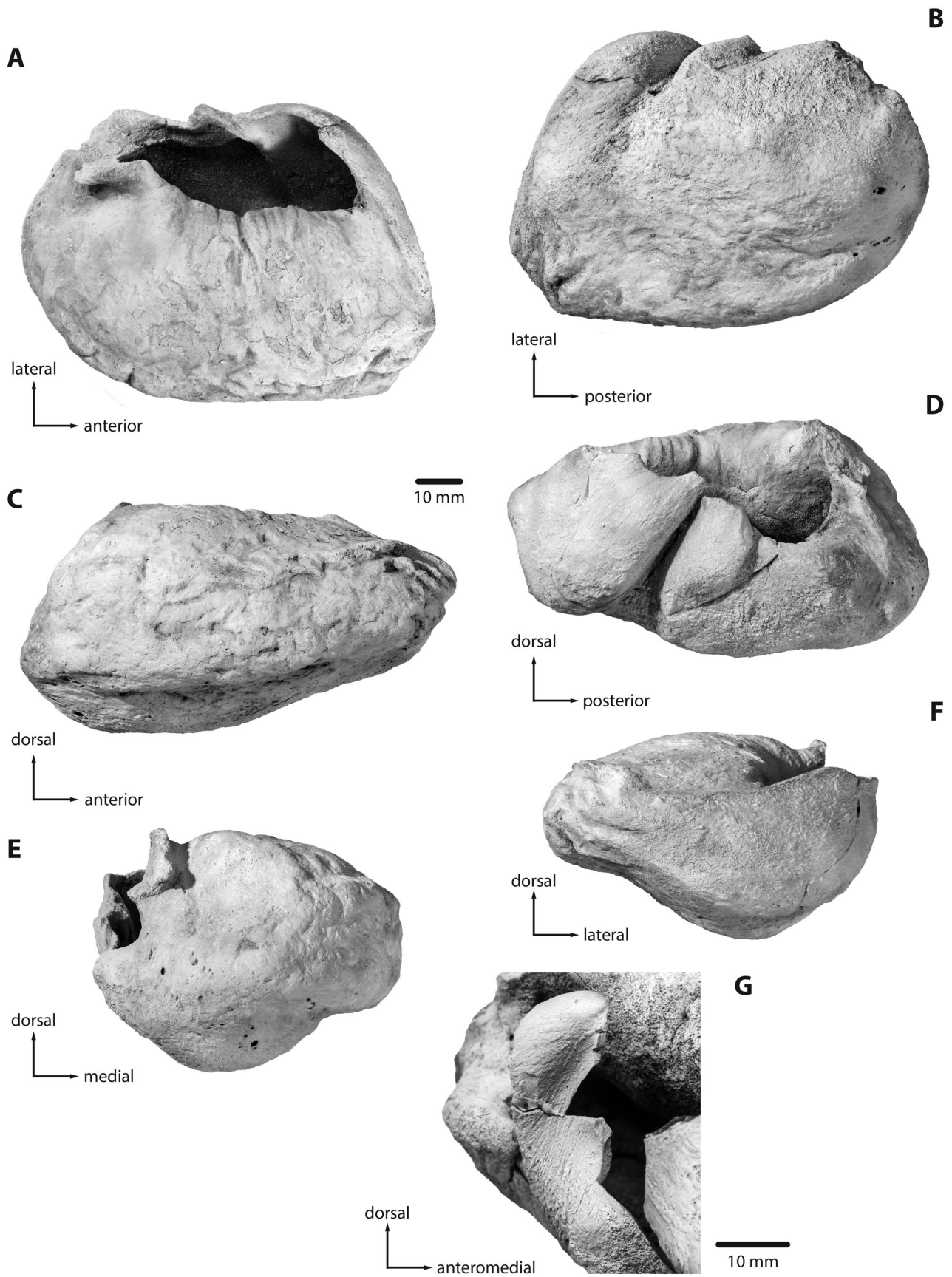
Figure 7. Holotype left tympanic bulla of *Antwerpibalaena liberatlas* (IRSNB M2325). Photographs in **A**, dorsal, **B**, ventral, **C**, medial, **D**, lateral, **E**, posterior and **F**, anterior views. **G**, photograph of the right sigmoid process in anterodorsolateral view.
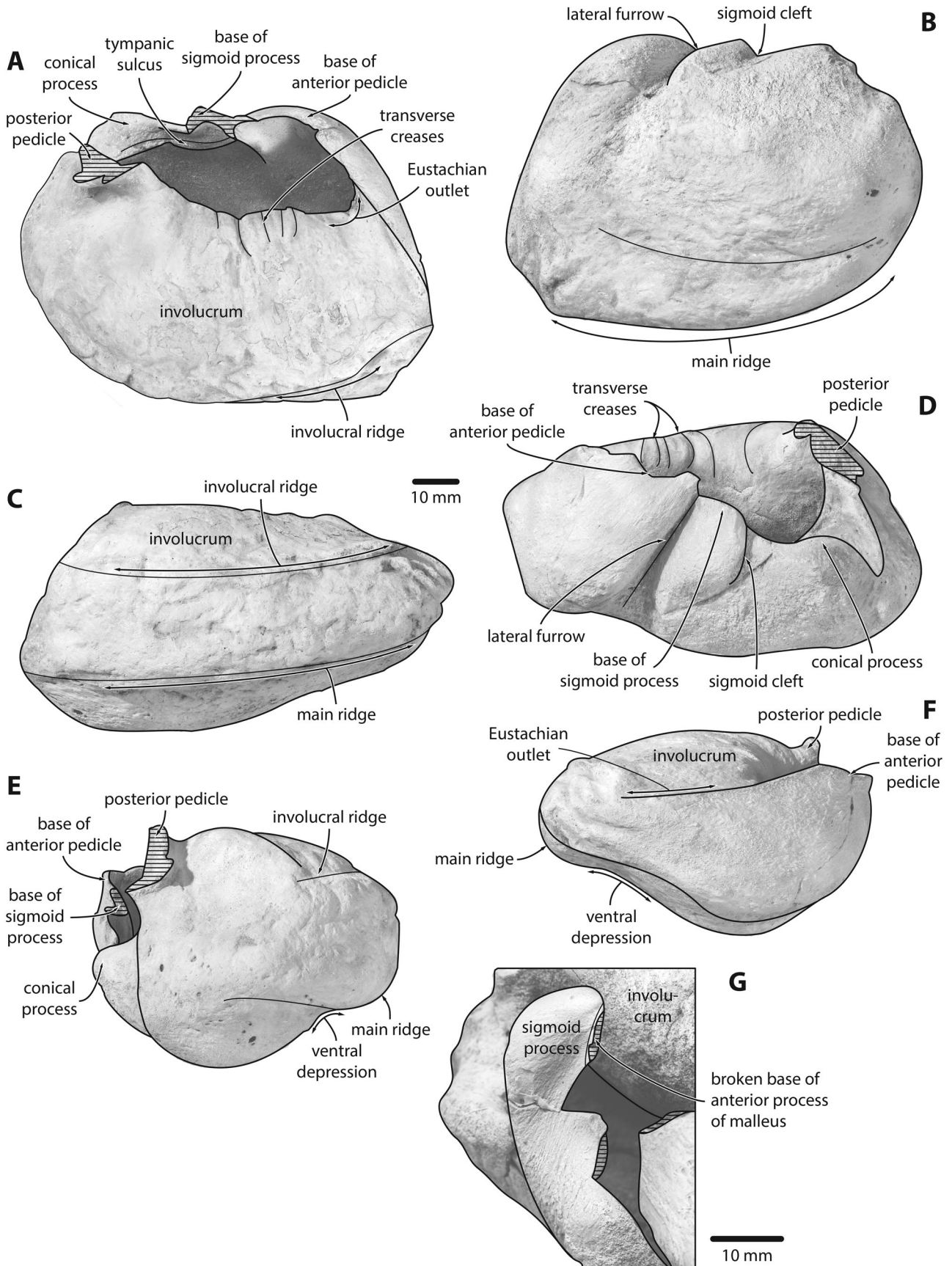
Figure 8. Holotype left tympanic bulla of *Antwerpibalaena liberatlas* (IRSNB M2325). Line drawings in **A**, dorsal, **B**, ventral, **C**, medial, **D**, lateral, **E**, posterior and **F**, anterior views. **G**, line drawing of the right sigmoid process in anterodorsolateral view. Hatched parts are broken.
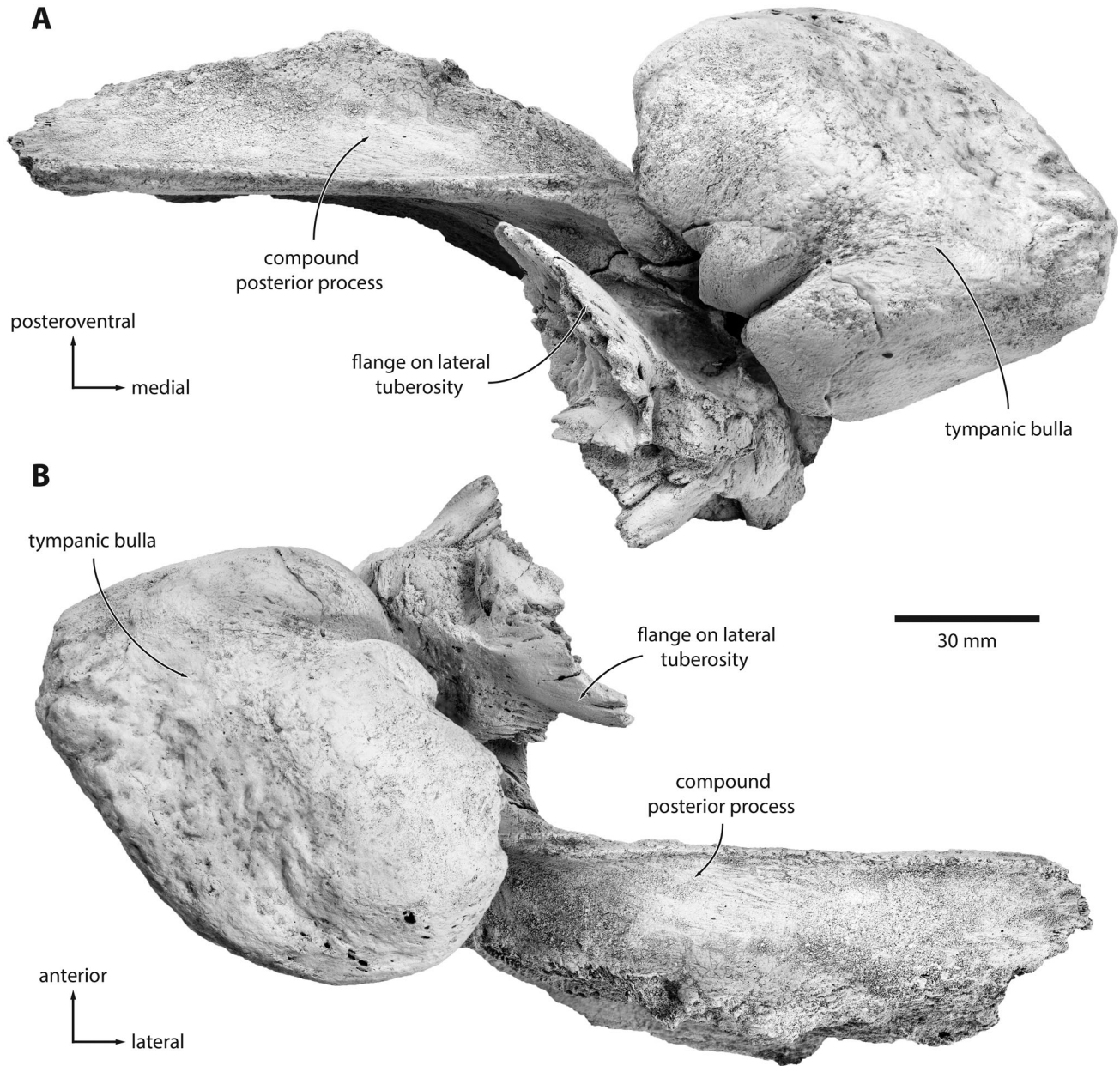
Figure 9. Articulated left ear bones of the holotype of *Antwerpibalaena liberatlas* (IRSNB M2325). Photographs in **A**, anteroventral and **B**, ventral views.

elongate and oriented medially, and terminates in a hook-shaped manubrium. The lenticular process of the incus is slender and clearly offset from the body. Other details are obscured by the arrangement of the ossicles and a thin concretionary layer remaining attached to the specimen.

Mandible
In dorsal view, the mandible is convex laterally, with a straight (rather than recurved) neck (Fig. 11). The medial surface of the body is flat, whereas its lateral side is strongly convex dorsoventrally. The anterior-most portion of the body is notably twisted (clockwise on the right, anticlockwise on the left), causing it to appear nearly horizontal. The symphysis is unsutured and marked by a long groove. In medial view, the coronoid process is reduced to a barely noticeable tuberosity. There is a well-defined mylohyoid groove running near and roughly parallel to the ventral border of the body. The angular process is massive and not deflected ventrally.
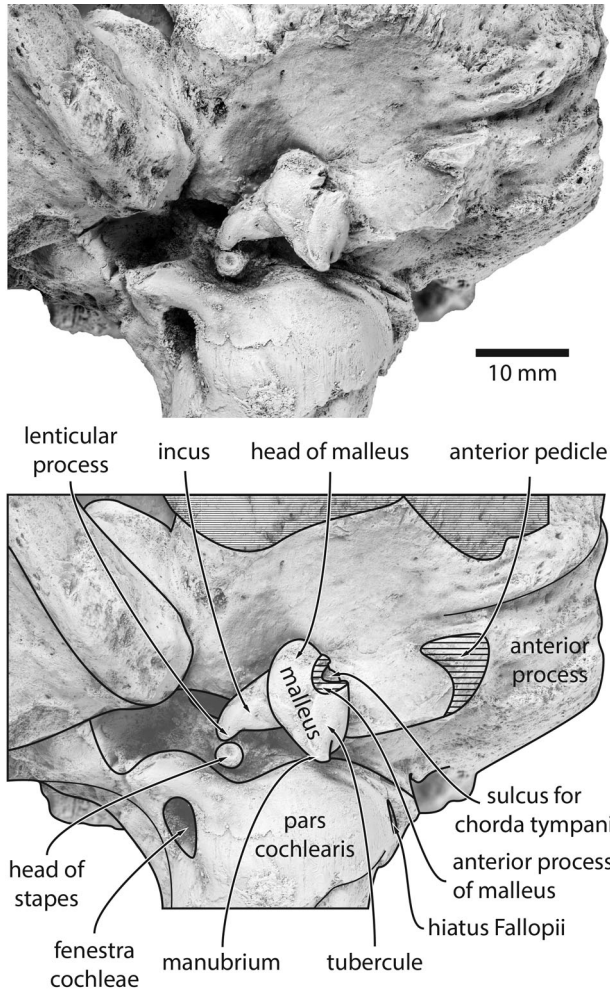
Figure 10. Photograph and line drawing of the *in situ* holotype right auditory ossicles of *Antwerpibalaena liberatlas* (IRSNB M2325), in ventral view.

Hyoid

In dorsal view, the basihyal and thyrohyals are firmly fused (Fig. 11). The thyrohyals are oriented slightly posterolaterally; in cross-section, they are somewhat flattened medially, but become more oval distally. As in extant balaenids, a broad but shallow anterior notch separates a pair of short and stocky anterior projections. Unlike in *Balaena* and *Eubalaena*, however, there are no posterior projections on the basihyal (Omura 1964).

Cervical vertebrae

All of the cervical vertebrae except the atlas are fused, with fusion affecting both the bodies and the transverse processes (Fig. 12). In anterior view, the confluent neural canal and odontoid fovea of the atlas are oval, with no obvious constriction as seen in *Balaenula*

balaenopsis and *Balaena ricei*. The condyloid facets are massive and well defined, whereas the neural and inferior arches are relatively gracile. The articular facets on the axis are rough and poorly defined. Its similarly sized upper and lower transverse processes enclose a large vertebrarterial foramen. In posterior view, the body of C7 is squared.

Thoracic vertebrae

There are five post-cervical vertebrae. Four of these are thoracics characterized by cordiform to rounded bodies, wide neural canals and robust transverse processes arising high on the neural arch, above the level of the body (Fig. 13). By contrast, the posterior-most vertebra (Fig. 13E) has horizontally directed, flattened transverse processes that arise from the centre of the oval body. This morphology is consistent with either a posterior thoracic or a lumbar vertebra. In the absence of a pronounced ventral keel, we preliminarily identify this vertebra as a posterior thoracic.

Forelimb

In lateral view, the scapula is fragmentary, but preserves a well-developed acromion and the base of the coracoid process (Fig. 14). The humerus is shorter than the radius and ulna. The radial and ulnar facets are oriented at an angle, implying the immobilization of the elbow. The head of the humerus is large and notably angled posteriorly, but less so than in extant balaenids. The humeral shaft is straight anteriorly but concave posteriorly; there is no deltoid crest. The ulna is slender and bears a tall olecranon process. A shallow angle in the anterior border of the radius is likely homologous with the radial tuberosity. There are six finger bones, all of them dumbbell shaped and, except for two, longer than wide (Fig. 14C). The largest of these bones likely represents a metacarpal, whereas the smallest three are almost certainly phalanges. The identification of the other elements remains ambiguous.

Sternum and ribs

In ventral view, the manubrium is pointed posteriorly and rounded anteriorly, thus forming a spade- or heart-like shape (Fig. 14D). Overall, the bone is flattened, with a weakly convex ventral surface and a correspondingly concave dorsal one. Laterally, there is a well-defined insertion for the first rib. The rib cage is relatively complete and comprises at least 11 ribs, although the original number was presumably somewhat higher (Fig. 15). In lateral view, all of
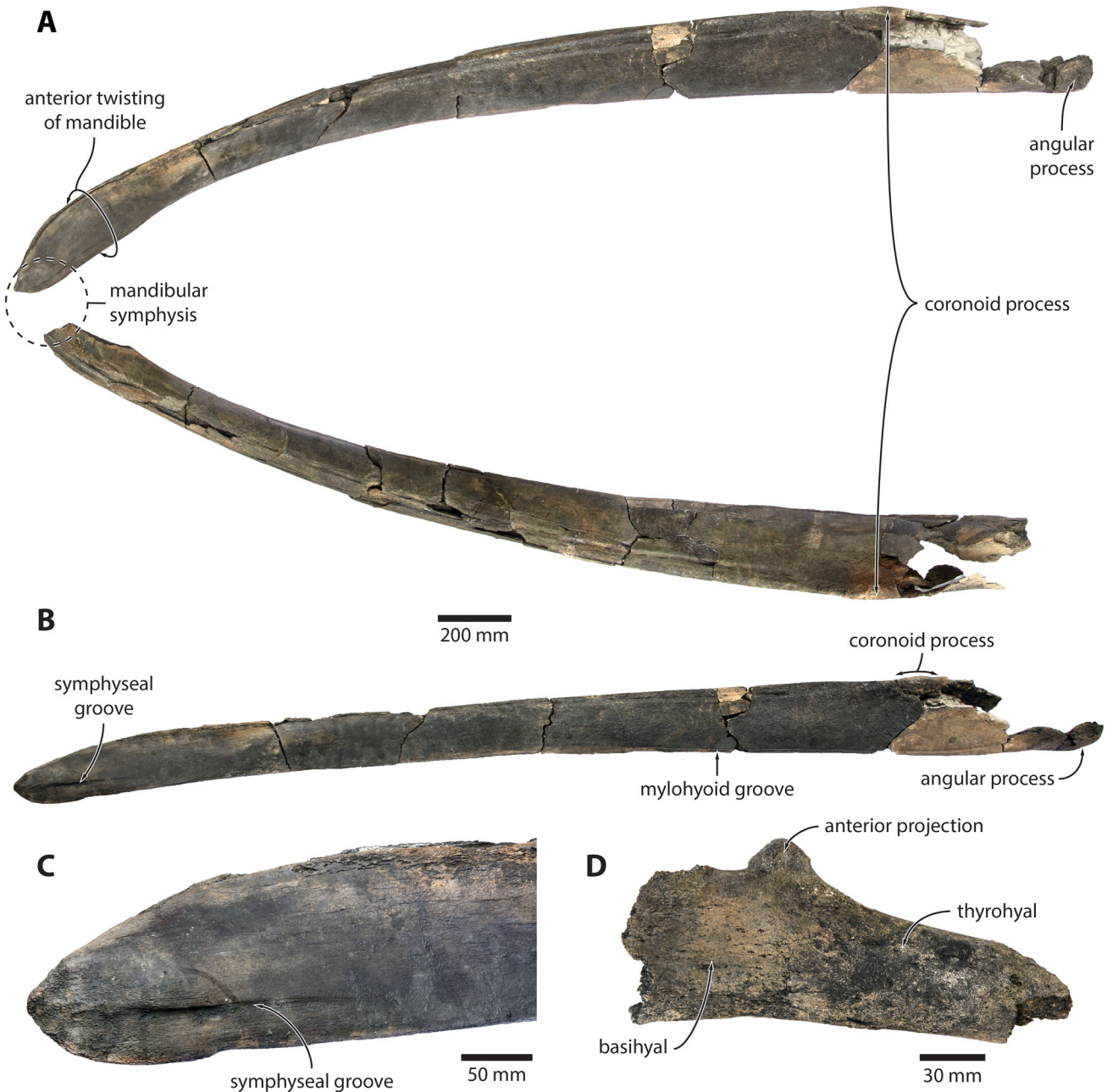
A

anterior twisting
of mandible

mandibular
symphysis

angular
process

coronoid process

B

200 mm

coronoid process

symphyseal
groove

mylohyoid groove

angular process

anterior projection

C

thyrohyal

D

basihyal

symphyseal groove   50 mm

30 mm

Figure 11. Holotype mandible and hyoid of *Antwerpibalaena liberatlas* (IRSNB M2325). **A**, mandibles in dorsal view. **B**, right mandible in medial view. **C**, symphyseal region of right mandible in medial view. **D**, fused basi- and thyrohyals in dorsal view.

the ribs are slender, as in all extant mysticetes except *Caperea*.

Discussion

Phylogeny

The results of the phylogenetic analysis strongly support balaenid monophyly (Figs 16, S1), with shared features including the lack of a re-entrant between the posterior border of the zygomatic process of the squamosal and the exoccipital (ch. 74); a posteriorly positioned orbito-temporal crest (ch. 76); a broad exposure of the frontal on the vertex (ch. 80); a parietal that is higher than long in lateral view (ch. 86); a tall squamosal (ch. 102) bearing a short squamosal fossa (ch. 106) and a dorsoventrally expanded zygomatic process (ch. 96) that is both twisted (ch. 99) and oriented anterolaterally (ch. 97); a rounded supraoccipital shield (ch. 112) with a flat or convex anterior portion (ch. 113); a ventrally oriented
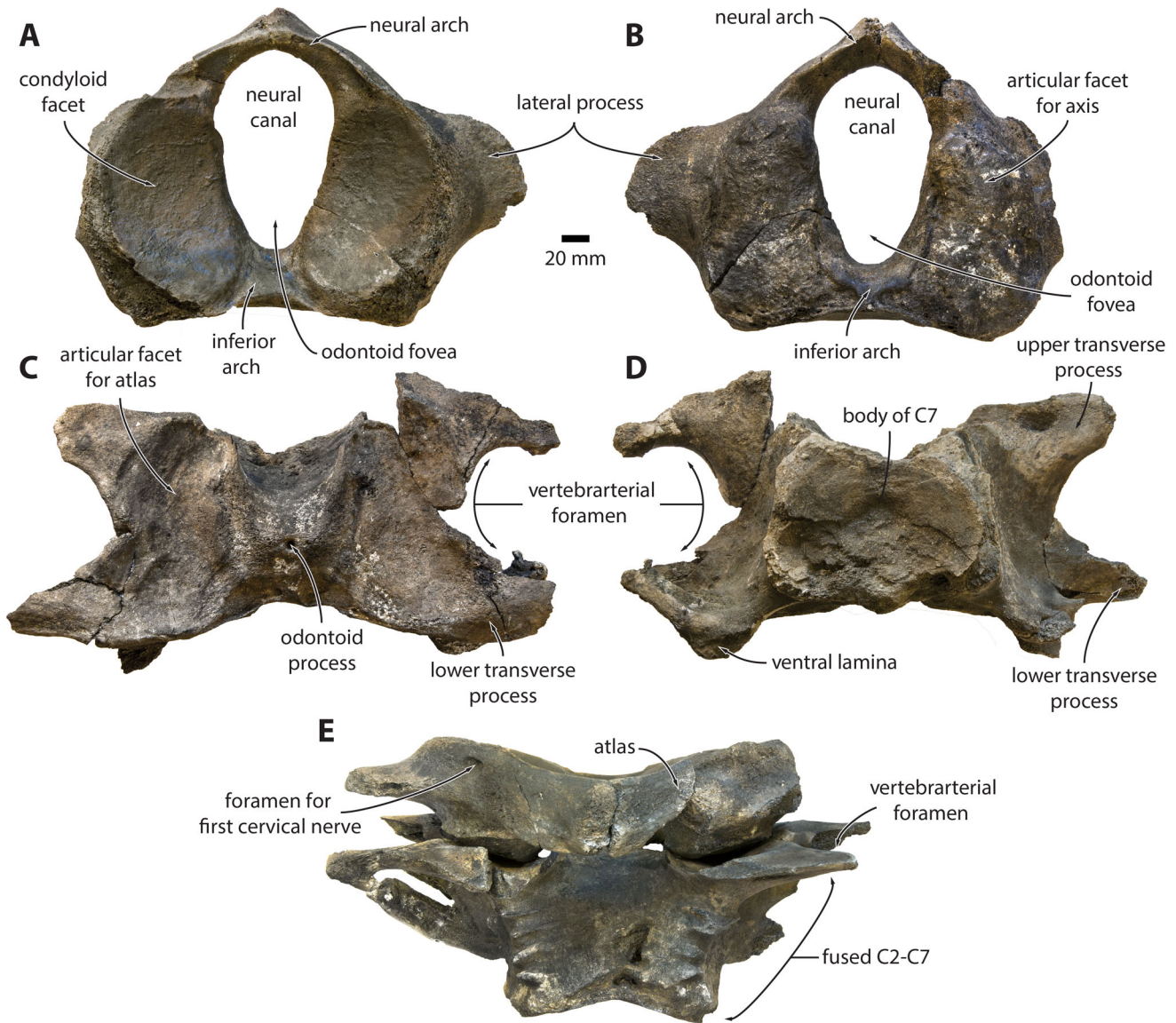
Figure 12. Holotype cervical vertebrae of *Antwerpibalaena liberatlas* (IRSNB M2325). Atlas in **A**, anterior and **B**, posterior views. Axis and remaining cervical vertebrae in **C**, anterior and **D**, posterior views. **E**, articulated cervical vertebrae in dorsal views.

(ch. 117) and parallel-sided (ch. 118) postglenoid process in posterior view; the presence of a ridge delimiting the dorsomedial border of the glenoid fossa on the squamosal (ch. 121); a posteriorly open foramen pseudovale (ch. 128); and a ventrally bulging posterior cochlear crest (ch. 166).

Within balaenids, *Morenocetus parvus* diverges first, followed by *Peripolocetus vexillifer* and *Balaenula* sp. from Japan. At this point, right whales seem to have split into a clade of small- to medium-sized species including *Antwerpibalaena*, *Balaenella* and *Balaenula astensis*, supported by a somewhat posteriorly positioned lateral furrow on the tympanic bulla (in lateral view; ch. 194); and a second clade of medium- to large-sized taxa

including *Balaena* and *Eubalaena*. Neither of these clades is well supported, however.

Balaenula appears to be polyphyletic, with the preliminarily described *Balaenula* sp. (Kimura 2009) being far more basal than *B. astensis*. The genus is based on *B. balaenopsis*, which in turn rests on a fragmentary and rather juvenile type specimen (IRSNB M0853a–f) from the Pliocene of Belgium (Van Beneden 1872, 1880; Abel 1941). Since its description in the late nineteenth century, *Balaenula* has sometimes been used as a catch-all for small balaenid fossils from across the globe (Van Beneden 1880; Barnes 1977; Oishi & Hasegawa 1995; Whitmore & Kaltenbach 2008). To clarify its content and scope, both the genus and its type species are in need of review.
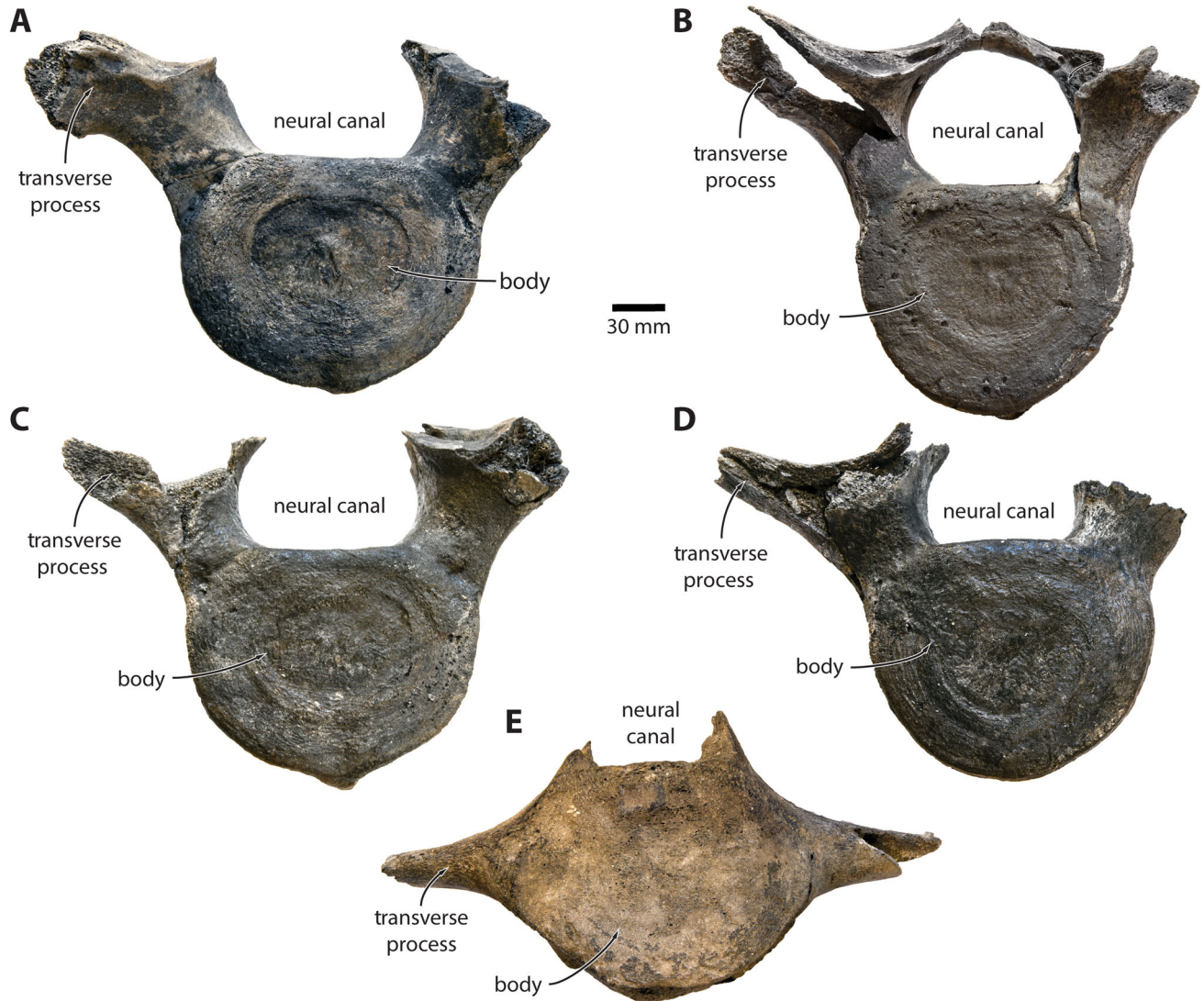
Figure 13. A–E, holotype thoracic vertebrae of *Antwerpibalaena liberatlas* (IRSNB M2325) in anterior views. The identification of the last vertebra (E) is tentative.

In line with molecular and total evidence studies (Steeman *et al.* 2009; Fordyce & Marx 2013; Gol'din & Steeman 2015; Marx & Fordyce 2015; Buono *et al.* 2017; McGowen *et al.* 2019), but contrary to most morphological analyses (Bouetel & de Muizon 2006; Steeman 2007; Churchill *et al.* 2012; El Adli *et al.* 2014; Bisconti 2015; Boessenecker & Fordyce 2015; Bisconti *et al.* 2019), *Caperea marginata* is recovered as a plicogulan (Cetotheriidae + Balaenopteridae), rather than as sister to balaenids. This result is further informed by the morphology of the cervical complex of *Antwerpibalaena*.

Complete fusion of the cervical vertebrae (i.e. C1–C7) is a defining feature of extant balaenids, and often considered one of the primary features uniting *Caperea* with right whales (Bisconti 2012; El Adli *et al.* 2014; Bisconti *et al.* 2017). This inference, however, is based on

relatively few data. Within Balaenidae, complete cervical fusion has so far only been confidently demonstrated for *Balaena* and *Eubalaena* (Omura *et al.* 1969; Westgate & Whitmore 2002; Bisconti 2003). By contrast, the neck of more basal taxa either remains unknown (*Morenocetus*, *Peripolocetus*) or shows only partial fusion (e.g. *Balaenula*), with the atlas and C7 either fusing late during ontogeny or perhaps not at all (Van Beneden 1880; Whitmore & Kaltenbach 2008). Abel (1941) interpreted this pattern as an evolutionary trend within right whales, thus calling into question the validity of fused cervicals as a universal balaenid feature.

Until now, Abel's idea has gained little traction, presumably because the specimens he studied were juvenile and, in some cases, uncertainly associated. *Antwerpibalaena* rectifies these issues, and demonstrates
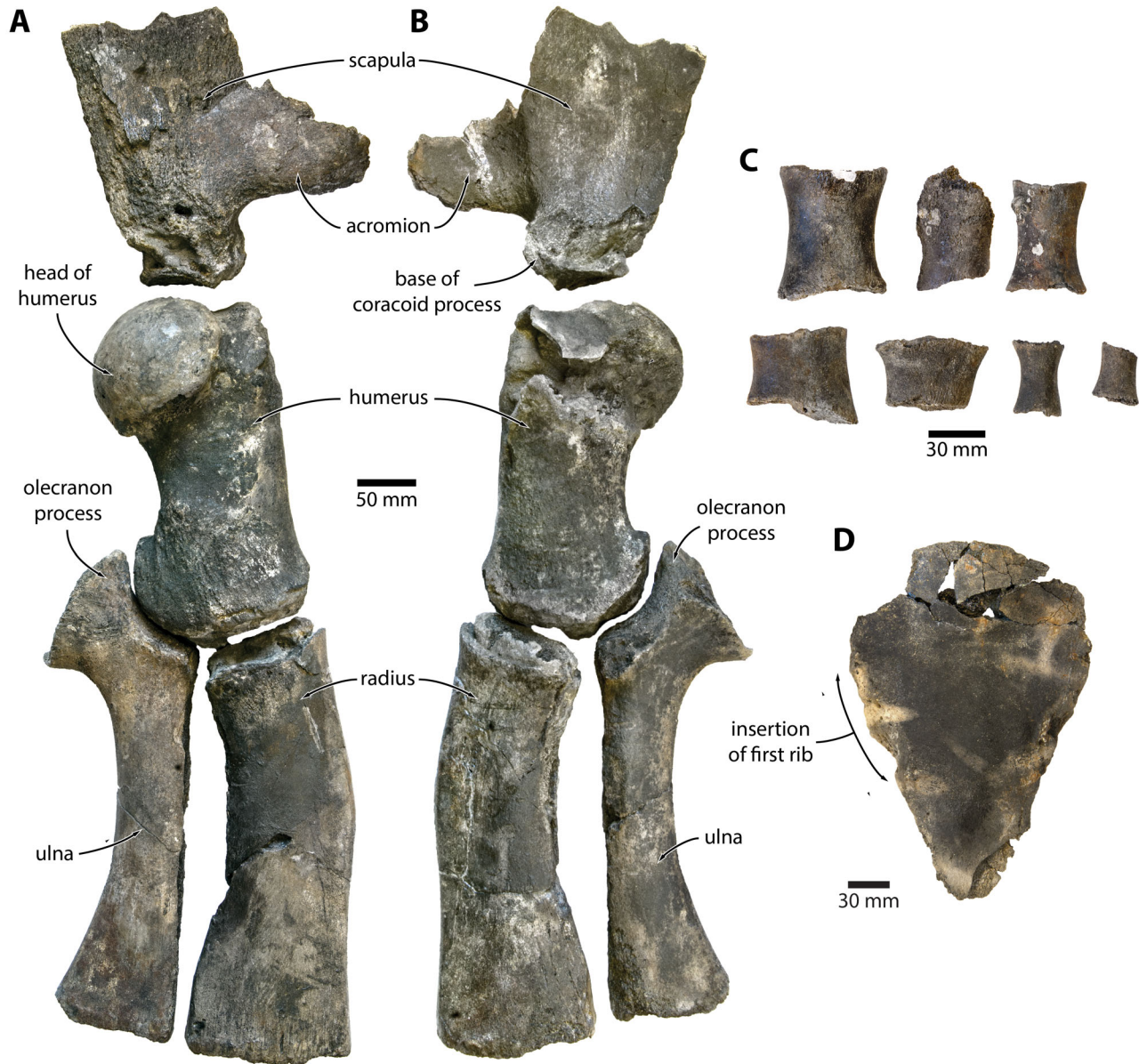
Figure 14. Holotype forelimb and sternum of *Antwerpibalaena liberatlas* (IRSNB M2325). Right forelimb (scapula, humerus, radius and ulna) in **A**, lateral and **B**, medial views. **C**, finger bones, including a presumed metacarpal (top left). **D**, sternum in ventral view.

that partial cervical fusion genuinely occurred in adults of at least one extinct right whale. Crucially, this interpretation implies that complete fusion was either achieved independently by balaenids and *Caperea* or secondarily lost in at least one species, thus weakening the case for a sister-group relationship.

Balaenid body size evolution

The estimated bizygomatic width of *Antwerpibalaena*, as inferred from the right half of the skull, is 1.1–1.2 m, which in turn suggests a total body length of 9.5–11.9

m. These results are consistent with the length of the mandible, which in extant right whales contributes approximately one-quarter to one-third of the total body length (Tomilin 1957), and thus implies a length of 7.8–10.4 m for *Antwerpibalaena*. Overall, these estimates make it comparable to *Balaenula* sp. from northern Japan (9.3–9.5 m), but larger than *Balaenula*, *Balaenella*, *Morenocetus* and *Peripolocetus* (5–8 m), and smaller than the extant balaenids (Excavation Research Group for the Fukagawa Whale Fossil 1982; Bisconti *et al.* 2017; Buono *et al.* 2017; Slater *et al.* 2017).

Figure 15. Holotype ribs of *Antwerpibalaena liberatlas* (IRSNB M2325) in anterior view (left ribs on top).

The intermediate size of *Antwerpibalaena* adds to an increasingly complex picture of balaenid body size evolution. The earliest right whales, *Morenocetus* and *Peripolocetus*, were rather small, with a total body length of 5–6 m (Bisconti *et al.* 2017; Buono *et al.* 2017). By the late Miocene, some species had achieved much larger sizes, as demonstrated by *Eubalaena shinshuensis* (12–13 m) (Kimura 2009). There was not, however, a simple trend from small to large across the entire family. Instead, the relatively basal phylogenetic position and intermediate size of *Antwerpibalaena* and *Balaenula* sp. suggest that some Pliocene right whales (e.g. *Balaenula* and *Balaenella*) secondarily reverted to smaller body sizes. Better-supported phylogenies and additional data from the poorly sampled Miocene are needed to test this hypothesis.

Evolution of the balaenid flipper

Extant mysticete flipper shapes fall into two main categories: broad and paddle-like in right whales and grey whales, where they are thought to increase low-speed manoeuvrability; and narrow and elongate in *Caperea* and rorquals, where they may be associated with high-speed swimming (Benke 1993; Cooper *et al.* 2007). Compared to extant balaenids, *Antwerpibalaena* has a better-developed acromion process, a less obviously flared distal epiphysis of the ulna, and a notably smaller and less inclined humeral head (Fig. 17). In addition, it differs especially from *Eubalaena* in having a relatively longer forearm. Together, these characteristics imply a comparatively slender flipper with a smaller range of motion. *Antwerpibalaena* thus documents previously unseen variability in balaenid flipper
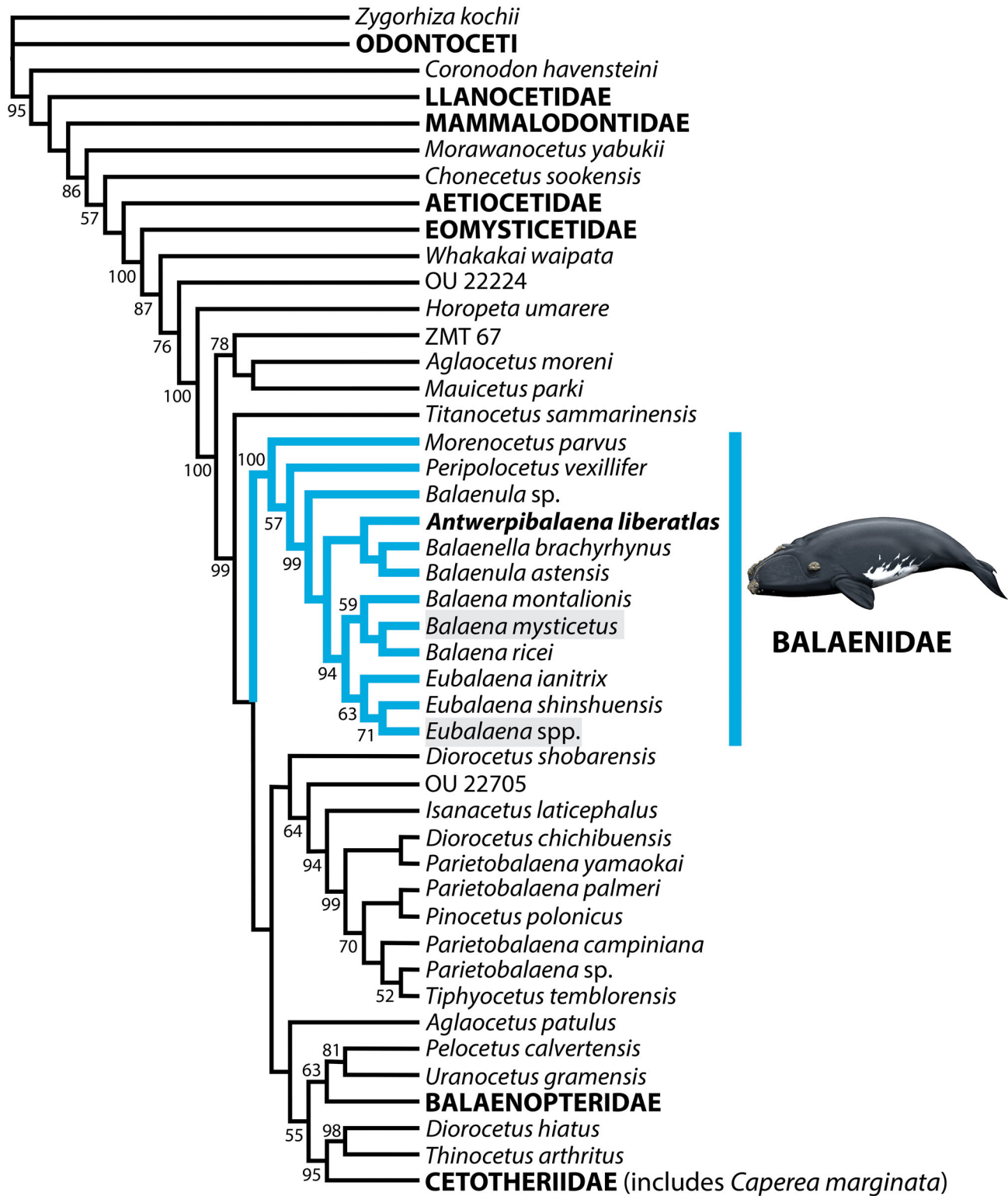
Figure 16. Consensus tree showing all compatible groups arising from the Bayesian total evidence (molecular + morphological data) analysis. Numbers next to nodes represent posterior probabilities, values below 50 are not shown. Grey shading within Balaenidae indicates extant species. Drawing of whale by Carl Buell.
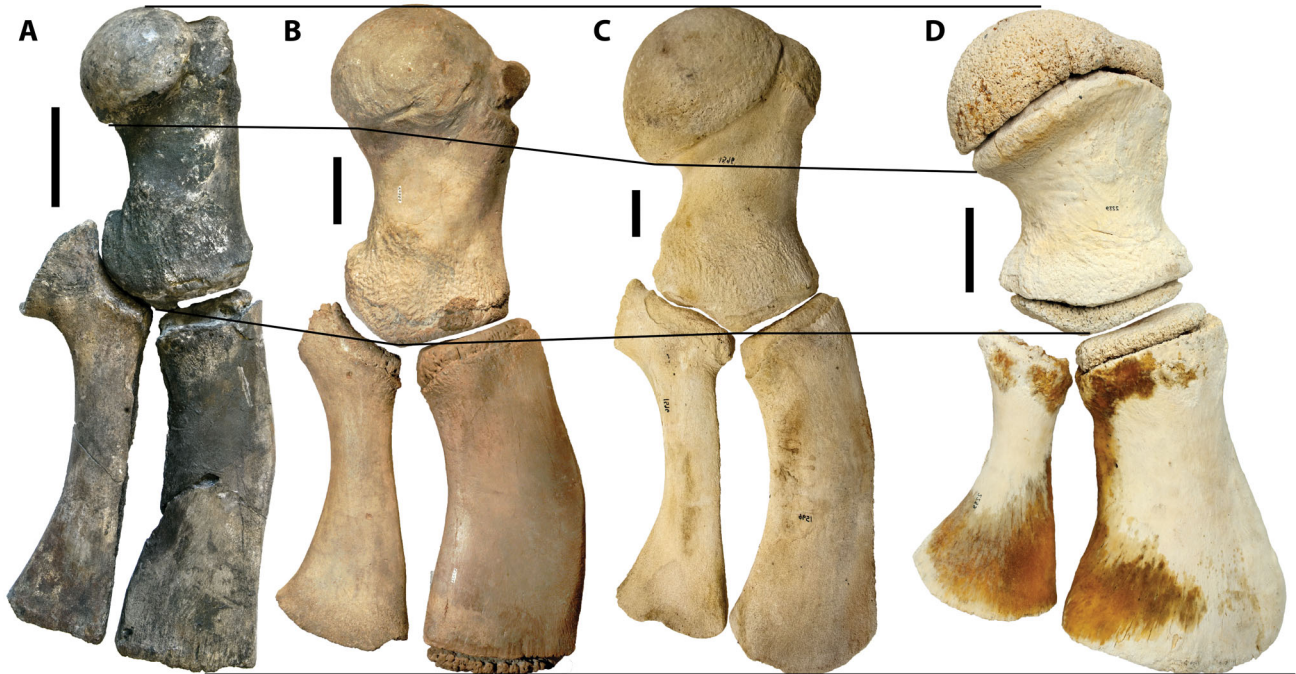
Figure 17. Comparison of the forelimb of **A**, *Antwerpibalaena liberatlas* (IRSNB M2325), **B**, *Balaena ricei* (USNM 22553), **C**, *Balaena mysticetus* (ZMUC 1596); and **D**, *Eubalaena australis* (NMNZ MM002239). Scale bars = 100 mm. Photo of NMNZ MM002239 by R. E. Fordyce.

shape, which plausibly correlates with different locomotory styles.

Also notable are the dimensions of the finger bones, at least two of which are wider than long. This foreshortening appears inconsistent with the relatively elongate arm bones of *Antwerpibalaena*, and generally is atypical for mysticetes. By contrast, short finger bones do occur in some odontocetes like the killer whale, *Orcinus orca* (Cooper *et al.* 2007). The preservation, size and association of these elements with the remainder of the skeleton give us no *a priori* reason to doubt their identification as part of the holotype. Nevertheless, given their unusual anatomy we refrain from interpreting them further here, until their identity can be confirmed via additional specimens.

The Belgian right whale assemblage

Insights from Belgian fossils have in the past been hindered by a lack of clear locality data and dubious specimen associations (Steeman 2010). By contrast, more recent work has demonstrated the potential of the local record to provide a detailed window into cetacean evolution at a time of pronounced global change (Bisconti 2005; Lambert & Gigase 2007; Bisconti *et al.* 2019; Marx *et al.* 2019).

Antwerpibalaena adds to the diversity of the Belgian assemblage and confirms the occurrence of a disparate range of balaenids – small, intermediate and large – in the Pliocene North Sea (Bisconti 2005; Bisconti *et al.* 2017). Further work is required to sift through the abundance of existing material to redefine poorly circumscribed species such as *Balaenula balaenopsis*, *Balaenotus insignis* and *Balaena primigenia* (Van Beneden 1880; Bisconti 2003). Overall, however, it appears that right whales were until recently far more ecologically diverse, and perhaps far more abundant, than their living kin. This reflects similar findings from the western North Atlantic and beyond (Westgate & Whitmore 2002; Whitmore & Kaltenbach 2008; Kimura 2009), and lends support to the existence of a marked Pliocene turnover event that defined the modern marine mammal fauna (Pimiento *et al.* 2017).

Conclusions

Antwerpibalaena liberatlas is a new, medium-sized (9.5–11.9 m) extinct balaenid from the Pliocene of Belgium. Its well-preserved postcranial remains provide novel insights into the evolution of extant balaenid anatomy and function, such as the emergence of a fused neck and paddle-shaped flippers. Its total body length falls between that of extant right whales and most

extinct species, and points to a more complex pattern of body size evolution than previously thought. The Pliocene North Sea was home to a disparate balaenid assemblage, ranging from small species like *Balaenella brachyrhynus* to comparative giants like *Eubalaena ianitrix*. Despite its chequered history, the Belgian Pliocene fossil record holds great potential to illuminate cetacean evolution at a time of major global change.

Supplemental data

Acknowledgements

ORCID

Stijn Goolaerts http://orcid.org/0000-0002-7082-9012
Travis Park http://orcid.org/0000-0002-9492-8859
Olivier Lambert http://orcid.org/0000-0003-0740-5791
Felix G. Marx http://orcid.org/0000-0002-1029-4001

References

Abel, O. 1938. Vorläufige Mitteilungen über die Revision der fossilen Mystacoceten aus dem Tertiaer Belgiens. *Bulletin du Musée Royal D'Histoire Naturelle de Belgique*, **14**, 1–34.

Abel, O. 1941. Vorläufige Mitteilungen über die Revision der fossilen Mystacoceten aus dem Tertiaer Belgiens (Zweiter Bericht). *Bulletin du Musée Royal D'Histoire Naturelle de Belgique*, **17**, 1–29.

Barnes, L. G. 1977. Outline of Eastern North Pacific fossil cetacean assemblages. *Systematic Zoology*, **25**, 321–343. doi:10.2307/2412508

Benke, H. 1993. Investigations on the osteology and functional morphology of the flipper of whales and dolphins. *Investigations on Cetacea*, **24**, 9–252.

Berta, A. & **Deméré, T. A.** 2017. Baleen whales, evolution. Pp. 69–75 in B. Würsig, J. G. M. Thewissen & K. M. Kovacs (eds) *Encyclopedia of marine mammals*. Academic Press, London.

Bisconti, M. 2003. Evolutionary history of Balaenidae. *Cranium*, **20**, 9–50.

Bisconti, M. 2005. Skull morphology and phylogenetic relationships of a new diminutive balaenid from the lower Pliocene of Belgium. *Palaeontology*, **48**, 793–816. doi:10.1111/j.1475-4983.2005.00488.x

Bisconti, M. 2012. Comparative osteology and phylogenetic relationships of *Miocaperea pulchra*, the first fossil pygmy right whale genus and species (Cetacea, Mysticeti, Neobalaenidae). *Zoological Journal of the Linnean Society*, **166**, 876–911. doi:10.1111/j.1096-3642.2012.00862.x

Bisconti, M. 2015. Anatomy of a new cetotheriid genus and species from the Miocene of Herentals, Belgium, and the phylogenetic and palaeobiogeographical relationships of Cetotheriidae s. s. (Mammalia, Cetacea, Mysticeti). *Journal of Systematic Palaeontology*, **13**, 377–395. doi:10.1080/14772019.2014.890136

Bisconti, M., **Lambert, O.** & **Bosselaers, M.** 2017. Revision of '*Balaena*' *belgica* reveals a new right whale species, the possible ancestry of the northern right whale, *Eubalaena glacialis*, and the ages of divergence for the living right whale species. *PeerJ*, **5**, e3464. doi:10.7717/peerj.3464

Bisconti, M., **Munsterman, D. K.** & **Post, K.** 2019. A new balaenopterid whale from the late Miocene of the southern North Sea Basin and the evolution of balaenopterid diversity (Cetacea, Mysticeti). *PeerJ*, **7**, e6915. doi:10.7717/peerj.6915

Boessenecker, R. W. & **Fordyce, R. E.** 2015. Anatomy, feeding ecology, and ontogeny of a transitional baleen whale, a new genus and species of Eomysticetidae (Mammalia: Cetacea) from the Oligocene of New Zealand. *PeerJ.* **3**, e1129. doi:10.7717/peerj.1129

Bosselaers, M., **Herman, J.**, **Hoedemakers, K.**, **Lambert, O.**, **Marquet, R.** & **Wouters, K.** 2004. Geology and palaeontology of a temporary exposure of the late Miocene Deurne Sand Member in Antwerpen (N. Belgium). *Geologica Belgica*, **7**, 27–39.

Bouetel, V. & **de Muizon, C.** 2006. The anatomy and relationships of *Piscobalaena nana* (Cetacea, Mysticeti), a Cetotheriidae s.s. from the early Pliocene of Peru. *Geodiversitas*, **28**, 319–395.

Brisson, M. J. 1762. *Regnum animale in classes IX distributum, sive synopsis methodica sistens generalem animalium distributionem in classes IX, & duarum primarum classium, quadripedum scilicet & cetaceorum, particularum divisionem in ordines, sectiones, genera, & species*. Theodorum Haak, Lugduni Batavorum, Leiden, 296 pp.

Buono, M. R., **Fernández, M. S.**, **Cozzuol, M. A.**, **Cuitiño, J. I.** & **Fitzgerald, E. M. G.** 2017. The early Miocene balaenid *Morenocetus parvus* from Patagonia (Argentina) and the evolution of right whales. *PeerJ*, **5**, e4148. doi:10.7717/peerj.4148

Churchill, M., **Berta, A.** & **Deméré, T. A.** 2012. The systematics of right whales (Mysticeti, Balaenidae). *Marine Mammal Science*, **28**, 497–521. doi:10.1111/j.1748-7692.2011.00504.x

Cione, A. L., **Cozzuol, M. A.**, **Dozo, M. T.** & **Acosta Hospitaleche, C.** 2011. Marine vertebrate assemblages in the southwest Atlantic during the Miocene. *Biological Journal of the Linnean Society*, **103**, 423–440. doi:10.1111/j.1095-8312.2011.01685.x

Colpaert, W., **Bosselaers, M.** & **Lambert, O.** 2015. Out of the Pacific: a second fossil porpoise from the Pliocene of the North Sea Basin. *Acta Palaeontologica Polonica*, 60(1), 1–10. doi:http://dx.doi.org/10.4202/app.00115.2014

Cooper, L. N., **Berta, A.**, **Dawson, S. D.** & **Reidenberg, J. S.** 2007. Evolution of hyperphalangy and digit reduction in the cetacean manus. *The Anatomical Record*, **290**, 654–672. doi:10.1002/ar.20532

De Schepper, S., **Head, M. J.** & **Louwye, S.** 2009. Pliocene dinoflagellate cyst stratigraphy, palaeoecology and sequence stratigraphy of the Tunnel-Canal Dock, Belgium. *Geological Magazine*, **146**, 92–112. doi:10.1017/S0016756808005438

Deméré, T. A. & **Pyenson, N. D.** 2015. Filling the Miocene 'balaenid gap' – the previously enigmatic *Peripolocetus vexillifer K*ellogg, 1931 is a stem balaenid (Cetacea, Mysticeti) from the middle Miocene (Langhian) of California, USA. *Journal of Vertebrate Paleontology, Program and Abstracts*, **2015**, 115.

Deméré, T. A., **McGowen, M. R.**, **Berta, A.** & **Gatesy, J.** 2008. Morphological andmysticete whales. *Systematic Biology*, **57**, 15–37. doi:10.1080/10635150701884632

Ekdale, E. G. 2016. Morphological variation among the inner ears of extinct and extant baleen whales (Cetacea: Mysticeti). *Journal of Morphology*, **277**, 1599–1615. doi:10.1002/jmor.20610

Ekdale, E. G. & **Racicot, R. A.** 2015. Anatomical evidence for low frequency sensitivity in an archaeocete whale: comparison of the inner ear of *Zygorhiza kochii* with that of crown Mysticeti. *Journal of Anatomy*, **226**, 22–39. doi:10.1111/joa.12253

El Adli, J. J., **Deméré, T. A.** & **Boessenecker, R. W.** 2014. *Herpetocetus morrowi* (Cetacea: Mysticeti), a new species of diminutive baleen whale from the upper Pliocene (Piacenzian) of California, USA, with observations on the evolution and relationships of the Cetotheriidae. *Zoological Journal of the Linnean Society*, **170**, 400–466. doi:10.1111/zoj.12108

Excavation Research Group for the Fukagawa Whale Fossil 1982. *Research report on the Pliocene Balaenula (Suborder Mysticoceti [sic]) collected from Fukagawa City, Hokkaido*. City Board of Education, Fukagawa City, 132 pp. [In Japanese with English summary].

Fitzgerald, E. M. G. 2004. A review of the Tertiary fossil Cetacea (Mammalia) localities in Australia. *Memoirs of Museum Victoria*, **61**, 183–208. doi:10.24199/j.mmv.2004.61.12

Fordyce, R. E. & **Marx, F. G.** 2013. The pygmy right whale *Caperea marginata*, the last of the cetotheres. *Proceedings of the Royal Society B: Biological Sciences*, **280**, 20122645. doi:10.1098/rspb.2012.2645

Fordyce, R. E. & **de Muizon, C.** 2001. Evolutionary history of cetaceans: a review. Pp. 169–233 in J.-M. Mazin & V. de Buffrénil (eds) *Secondary adaptation of tetrapods to life in water*. Verlag Dr. Friedrich Pfeil, München.

Fraser, F. C. & **Purves, P. E.** 1960. Hearing in cetaceans. *Bulletin of the British Museum (Natural History), Zoology*, **7**, 3–139.

Gaines, C. A., **Hare, M. P.**, **Beck, S. E.** & **Rosenbaum, H. C.** 2005. Nuclear markers confirm taxonomic status and relationships among highly endangered and closely related right whale species. *Proceedings of the Royal Society B*, **272**, 533–542. doi:10.1098/rspb.2004.2895

Geisler, J. H. & **Sanders, A. E.** 2003. Morphological evidence for the phylogeny of Cetacea. *Journal of Mammalian Evolution*, **10**, 23–129. doi:10.1023/A:1025552007291

Geisler, J. H., **McGowen, M. R.**, **Yang, G.** & **Gatesy, J.** 2011. A supermatrix analysis of genomic, morphological, and paleontological data from crown Cetacea. *BMC Evolutionary Biology*, **11**, 1–33. doi:10.1186/1471-2148-11-112

George, J. C., **Rugh, D.** & **Suydam, R.** 2017. Bowhead whale *Balaena mysticetus*. Pp. 133–135 in B. Würsig, J. G. M. Thewissen & K. M. Kovacs (eds) *Encyclopedia of marine mammals*. Academic Press, London.

Gol'din, P. & **Steeman, M. E.** 2015. From problem taxa to problem solver: a new Miocene family, Tranatocetidae, brings perspective on baleen whale evolution. *PLoS ONE*, **10**, e0135500. doi:10.1371/journal.pone.0135500

Gray, J. E. 1864. Notes on the whalebone-whales; with a synopsis of the species. *Annals And Magazine of Natural History*, **14**, 345–353.

Gray, J. E. 1821. On the natural arrangement of vertebrose animals. *London Medical Repository*, **15**, 296–310.

Kenney, R. D. 2017. Right whales *Eubalaena glacialis*, *E. japonica*, and *E. australis*. Pp. 817–822 in B. Würsig, J. G.M. Thewissen & K. M. Kovacs (eds) *Encyclopedia of marine mammals*. Academic Press, London.

Ketten, D. R. & **Wartzok, D.** 1990. Three-dimensional reconstructions of the dolphin ear. *NATO ASI Series A, Life Sciences*, **196**, 81–105.

Kimura, T. 2009. Review of the fossil balaenids from Japan with a re-description of *Eubalaena shinshuensis* (Mammalia, Cetacea, Mysticeti). *Quaderni Del Museo di Storia Naturale di Livorno*, **22**, 3–21.

Lambert, O. 2008a. A new porpoise (Cetacea, Odontoceti, Phocoenidae) from the Pliocene of the North Sea. *Journal of Vertebrate Paleontology*, **28**, 863–872.

Lambert, O. 2008b. Sperm whales from the Miocene of the North Sea: a re-appraisal. *Bulletin de L'Institut Royal Des Sciences Naturelles de Belgique: Sciences de la Terre*, **78**, 277–216.

Lambert, O. & **Gigase, P.** 2007. A monodontid cetacean from the early Pliocene of the North Sea. *Bulletin de l'Institut Royal des. Sciences Naturelles de Belgique: Sciences de la Terre*, **77**, 197–210.

Lambert, O., **Bianucci, G.**, **Post, K.**, **de Muizon, C.**, **Salas-Gismondi, R.**, **Urbina, M.** & **Reumer, J.** 2010. The giant bite of a new raptorial sperm whale from the Miocene epoch of Peru. *Nature*, **466**, 105–108. doi:10.1038/nature09067

Lambertsen, R. H., **Rasmussen, K. J.**, **Lancaster, W. C.** & **Hintz, R. J.** 2005. Functional morphology of the mouth of the bowhead whale and its implications for conservation. *Journal of Mammalogy*, **86**, 342–352. doi:10.1644/BER-123.1

Lewis, P. O. 2001. A likelihood approach to estimating phylogeny from discrete morphological character data. *Systematic Biology*, **50**, 913–925. doi:10.1080/106351501753462876

Louwye, S., **Head, M. J.** & **De Schepper, S.** 2004. Dinoflagellate cyst stratigraphy and palaeoecology of the Pliocene in northern Belgium, southern North Sea Basin. *Geological Magazine*, **141**, 353–378. doi:10.1017/S0016756804009136

Manoussaki, D., **Chadwick, R. S.**, **Ketten, D. R.**, **Arruda, J.**, **Dimitriadis, E. K.** & **O'Malley, J. T.** 2008. The influence of cochlear shape on low-frequency hearing. *Proceedings of the National Academy of Sciences USA*, **105**(16), 6162–6166.

Marx, F. G. & **Fordyce, R. E.** 2015. Baleen boom and bust: a synthesis of mysticete phylogeny, diversity and disparity. *Royal Society Open Science*, **2**, 140434. doi:10.1098/rsos.140434

Marx, F. G. & **Fordyce, R. E.** 2016. A link no longer missing: new evidence for the cetotheriid affinities of *Caperea*. *PLoS ONE*, **11**, e0164059. doi:10.1371/journal.pone.0164059

Marx, F. G., **Post, K.**, **Bosselaers, M.** & **Munsterman, D. K.** 2019. A large late Miocene cetotheriid (Cetacea, Mysticeti) from the Netherlands clarifies the status of Tranatocetidae. *PeerJ*, **7**, e6426. doi:10.7717/peerj.6426

McGowen, M. R., **Spaulding, M.** & **Gatesy, J.** 2009. Divergence date estimation and a comprehensive molecular tree of extant cetaceans. *Molecular Phylogenetics and Evolution*, **53**, 891–906. doi:10.1016/j.ympev.2009.08.018

McGowen, M. R., **Tsagkogeorga, G.**, **Álvarez-Carretero, S.**, **dos Reis, M.**, **Struebig, M.**, **Deaville, R.**, **Jepson, P. D.**, **Jarman, S.**, **Polanowski, A.**, **Morin, P. A.** & **Rossiter, S. J.** 2019. Phylogenomic resolution of the cetacean tree of life using target sequence capture. *Systematic Biology*. doi:10.1093/sysbio/syz068

McLeod, S. A., **Whitmore, F. C.** & **Barnes, L. G.** 1993. Evolutionary relationships and classification. Pp. 45–70 in J. J. Burns, J. J. Montague & C. J. Cowles (eds) *The bowhead whale.* Society of Marine Mammalogy, Lawrence.

Mead, J. G. & **Fordyce, R. E.** 2009. The therian skull: a lexicon with emphasis on the odontocetes. *Smithsonian Contributions to Zoology*, **627**, 1–248. doi:10.5479/si.00810282.627

Miller, M. A., **Pfeiffer, W.** & **Schwartz, T.** 2010. Creating the CIPRES Science Gateway for inference of large phylogenetic trees. *Proceedings of the Gateway Computing Environments Workshop (GCE), 14 Nov. 2010*, New Orleans, LA, 1–8. https://ieeexplore.ieee.org/document/5676129

Moran, M. M., **Bajpai, S.**, **George, J. C.**, **Suydam, R.**, **Usip, S.** & **Thewissen, J. G. M.** 2015. Intervertebral and epiphyseal fusion in the postnatal ontogeny of cetaceans and terrestrial mammals. *Journal of Mammalian Evolution*, **22**, 93–109. doi:10.1007/s10914-014-9256-7

Oishi, M. & **Hasegawa, Y.** 1995. Diversity of Pliocene mysticetes from eastern Japan. *The Island Arc*, **3**, 436–452. doi:10.1111/j.1440-1738.1994.tb00124.x

Omura, H. 1964. A systematic study of the hyoid bones in the baleen whales. *Scientific Reports of the Whales Research Institute, Tokyo*, **18**, 149–170.

Omura, H., **Ohsumi, S.**, **Takahisa, N.**, **Nasu, K.** & **Kasuya, T.** 1969. Black right whales in the North Pacific. *Scientific Reports of the Whales Research Institute, Tokyo*, **21**, 1–78.

Park, T., **Evans, A. R.**, **Gallagher, S. J.** & **Fitzgerald, E. M. G.** 2017a. Low-frequency hearing preceded the evolution of giant body size and filter feeding in baleen whales. *Proceedings of the Royal Society B*, **284**, 20162528. doi:10.1098/rspb.2016.2528

Park, T., **Marx, F. G.**, **Fitzgerald, E. M. G.** & **Evans, A. R.** 2017b. The cochlea of the enigmatic pygmy right whale *Caperea marginata* informs mysticete phylogeny. *Journal of Morphology*, **278**, 801–809. doi:10.1002/jmor.20674

Pimiento, C., **Griffin, J. N.**, **Clements, C. F.**, **Silvestro, D.**, **Varela, S.**, **Uhen, M. D.** & **Jaramillo, C.** 2017. The Pliocene marine megafauna extinction and its impact on functional diversity. *Nature Ecology & Evolution*, **1**, 1100–1106. doi:10.1038/s41559-017-0223-6

Piper, K. J., **Fitzgerald, E. M. G.** & **Rich, T. H.** 2006. Mesozoic to early Quaternary mammal faunas of Victoria, south-east Australia. *Palaeontology*, **49**, 1237–1262. doi:10.1111/j.1475-4983.2006.00595.x

Pivorunas, A. 1979. The feeding mechanisms of baleen whales. *American Scientist*, **67**, 432–440.

Pyenson, N. D. & **Sponberg, S. N.** 2011. Reconstructing body size in extinct crown Cetacea (Neoceti) using allometry, phylogenetic methods and tests from the fossil record. *Journal of Mammalian Evolution*, **18**, 269–288. doi:10.1007/s10914-011-9170-1

Ritsche, I. S., **Fahlke, J. M.**, **Wieder, F.**, **Hilger, A.**, **Manke, I.** & **Hampe, O.** 2018. Relationships of cochlear coiling shape and hearing frequencies in cetaceans, and the occurrence of infrasonic hearing in Miocene Mysticeti. *Fossil Record*, **21**, 33–45. doi:10.5194/fr-21-33-2018

Roman, J., **Estes, J. A.**, **Morissette, L.**, **Smith, C.**, **Costa, D.**, **McCarthy, J.**, **Nation, J. B.**, **Nicol, S.**, **Pershing, A.** & **Smetacek, V.** 2014. Whales as marine ecosystem engineers. *Frontiers in Ecology and the Environment*, **12**, 377–385. doi:10.1890/130220

Ronquist, F., **Teslenko, M.**, **van der Mark, P.**, **Ayres, D. L.**, **Darling, A.**, **Höhna, S.**, **Larget, B.**, **Liu, L.**, **Suchard, M. A.** & **Huelsenbeck, J. P.** 2012. MrBayes 3.2: efficient Bayesian phylogenetic inference and model choice across a large model space. *Systematic Biology*, **61**, 539–542. doi:10.1093/sysbio/sys029

Slater, G. J., **Goldbogen, J. A.** & **Pyenson, N. D.** 2017. Independent evolution of baleen whale gigantism linked to Plio–Pleistocene ocean dynamics. *Proceedings of the Royal Society B*, **284**, 20170546. doi:10.1098/rspb.2017.0546

Steeman, M. E. 2007. Cladistic analysis and a revised classification of fossil and recent mysticetes. *Zoological Journal of the Linnean Society*, **150**, 875–894. doi:10.1111/j.1096-3642.2007.00313.x

Steeman, M. E. 2010. The extinct baleen whale fauna from the Miocene–Pliocene of Belgium and the diagnostic cetacean ear bones. *Journal of Systematic Palaeontology*, **8**, 63–80. doi:10.1080/14772011003594961

Steeman, M. E., **Hebsgaard, M. B.**, **Fordyce, R. E.**, **Ho, S. Y. W.**, **Rabosky, D. L.**, **Nielsen, R.**, **Rahbek, C.**, **Glenner, H.**, **Sorensen, M. V.** & **Willerslev, E.** 2009. Radiation of extant cetaceans driven by restructuring of the oceans. *Systematic Biology*, **58**, 573–585. doi:10.1093/sysbio/syp060

Tomilin, A. G. 1957. *Mammals of the USSR and adjacent countries, Vol. 9, Cetacea*. Akademii Nauk SSSR, Moscow, 717 pp. [In Russian, translated by the Israel Program for Scientific Translations, Jerusalem, 1967].

Van Beneden, P.-J. 1872. Les Baleines fossiles d'Anvers. *Bulletins de l'Académie royale des sciences. Des Lettres et Des Beaux-Arts de Belgique*, **34**, 6–23.

Van Beneden, P.-J. 1880. Description des ossements fossiles des environs d'Anvers. Deuxième partie. Cétacés. Genres *Balaenula. Balaena et Balaenotus. Annales du Musée Royal D'Histoire Naturelle de Belgique*, **4**, 1–82.

Werth, A. J. & **Potvin, J.** 2016. Baleen hydrodynamics and morphology of cross-flow filtration in balaenid whale suspension feeding. *PLoS ONE*, **11**, e0150106. doi:10.1371/journal.pone.0150106

Westgate, J. W. & **Whitmore, F. C.** 2002. *Balaena ricei*, a new species of bowhead whale from the Yorktown Formation (Pliocene) of Hampton, Virginia. *Smithsonian Contributions to Paleobiology*, **93**, 295–312.

Whitmore, F. C. & **Kaltenbach, J. A.** 2008. Neogene Cetacea of the Lee Creek Phosphate Mine, North Carolina. *Virginia Museum of Natural History Special Publication*, **14**, 181–269.

Associate Editor: Pip Brewer